MUON TRIGGER STUB ALIGNMENT ALGORITHM FOR HL-LHC UPGRADE

An Undergraduate Research Scholars Thesis

by

JOSE ROBERTO DIMAS VALLE

Submitted to Honors and Undergraduate Research
Texas A&M University
in partial fulfillment of the requirements for the designation as an

UNDERGRADUATE RESEARCH SCHOLAR

Approved by
Research Advisor: Prof. Alexei Safonov

May 2015

Major: Physics and Astronomy

TABLE OF CONTENTS

Page

ABSTRACT 1

NOMENCLATURE 2

ACKNOWLEDGMENTS 3

CHAPTER

I INTRODUCTION 4

II MUON DETECTOR OF CMS EXPERIMENT AT THE LHC 13

CMS Coordinate System 13

CMS Muon Detector 17

CMS Muon Trigger 21

III DT LOCAL TRIGGER RECONSTRUCTION 24

Bunch and Track Identifier 24

Track Correlator 26

Trigger Server 29

Sector Collector 30

IV DT MUON TRIGGER TRACK FINDER RECONSTRUCTION AND MOMENTUM MEASUREMEMENT 31

The Extrapolation Unit 32

The Track Assembler Unit 34

The Assignment Unit 35

V STUB ALIGNMENT ALGORITHM FOR THE UPGRADED CMS MUON TRIGGER 39

Shortcoming of the Current Implementation..... 41
Stub Alignment Algorithm Description 46
Findings 51

VI CONCLUSIONS AND OUTLOOK 54

REFERENCES 55

ABSTRACT

Muon Trigger Stub Alignment Algorithm for HL-LHC Upgrade. (May 2015)

Jose Roberto Dimas Valle
Department of Physics and Astronomy
Texas A&M University

Research Advisor: Prof. Alexei Safonov
Department of Physics and Astronomy

The high-luminosity upgrade of the Large Hadron Collider (HL-LHC) scheduled for 2022-2023 focuses on increasing the intensity of proton beams to produce a higher number of collisions per second. This upgrade will allow us to collect large amount of data needed for the studies on the Higgs sector and search for new phenomena. The upgrade also includes improvements on the detectors sensitivity to rare processes presenting signs of new physics, which could hold keys to the origins of dark matter and baryon asymmetry in the Universe, non-vanishing neutrino mass and many other phenomena not explained by the Standard Model. However, the increase in the density and rate of particles traversing particle detectors, including the CMS experiment at the LHC, imposes a challenge for high efficiency triggering. Trigger is the system responsible for ultra-fast online selection of potentially interesting data to diminish the rate of data to the level at which the data can be written to disk for offline analysis. The proposed upgrade of the CMS tracking system to acquire triggering capabilities is expected to address some of these difficulties, but a whole class of possible processes signifying presence of new physics via decays of long lived particles may become inaccessible to CMS. We propose and investigate a conceptually new trigger algorithm for reconstructing and measuring momenta of displaced muons using information from muon spectrometers only, which can be implemented as part of the re-design of the CMS Level-1 muon trigger for the HL-LHC to maintain CMS sensitivity to signatures with displaced muons.

ACKNOWLEDGMENTS

I would like to acknowledge Dr. Alexei Safonov and Dr. Vyacheslav Krutelyov for their support and guidance on the completion of this Undergraduate Research Scholars Thesis.

Dr. Duncan MacKenzie for his commitment and devotion in projects involving undergraduate students and for his successful leadership of the Undergraduate Research Scholars Program.

Special thanks to Aysen Tatarinov, Sven Dildick and Tao Huang for all of their help during my research.

NOMENCLATURE

LHC	Large Hadron Collider
HL LHC	High Luminosity Large Hadron Collider
CMS	Compact Muon Solenoid Experiment
CERN	Organisation Européenne pour la Recherche Nucléaire (European Organization for Nuclear Research)
DT	Drift Tubes
CSC	Cathode Strip Chambers
RPC	Resistive Plate Chambers
GEM	Gas Electron Multiplier

CHAPTER I

INTRODUCTION

The Standard Model of particle physics (SM) explains the interactions of known subatomic particles. It accounts for electromagnetic, weak and strong interactions but fails to describe gravitation as a quantum field theory. However, the contribution from the force or gravity is almost completely negligible at atomic scales [1].

Fig. I.1 shows the classification of elementary particles as bosons, quarks and leptons. Bosons are integer spin particles. They act as carriers of the fundamental forces, allowing leptons and quarks to interact with each other. Fermions are half integer spin particles that are not allowed to have the same quantum numbers within a system. They are further classified as quarks and leptons.

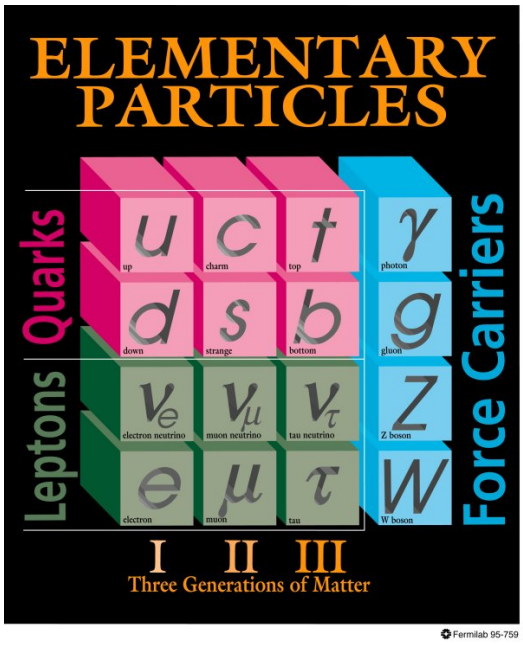

Fig. I.1. Elementary particles: leptons, quarks and gauge bosons [2].

Quarks interact via the strong force that glues them together in a composite particle, a hadron. Hadrons can be classified as baryons or mesons depending on the number of quark constituents. Leptons interact via the weak force, and all electrically charged particles participated in electromagnetic interactions. Electrons are perhaps the most well known example because of their role in chemical reactions.

Among the successes of the Standard Model are the prediction of neutrinos, muons, W and Z gauge bosons and the Higgs boson. Fig. I.2 shows a very powerful visual evidence of the existence of Higgs boson manifested by the excess of 4 lepton events with the invariant mass of 126 GeV.

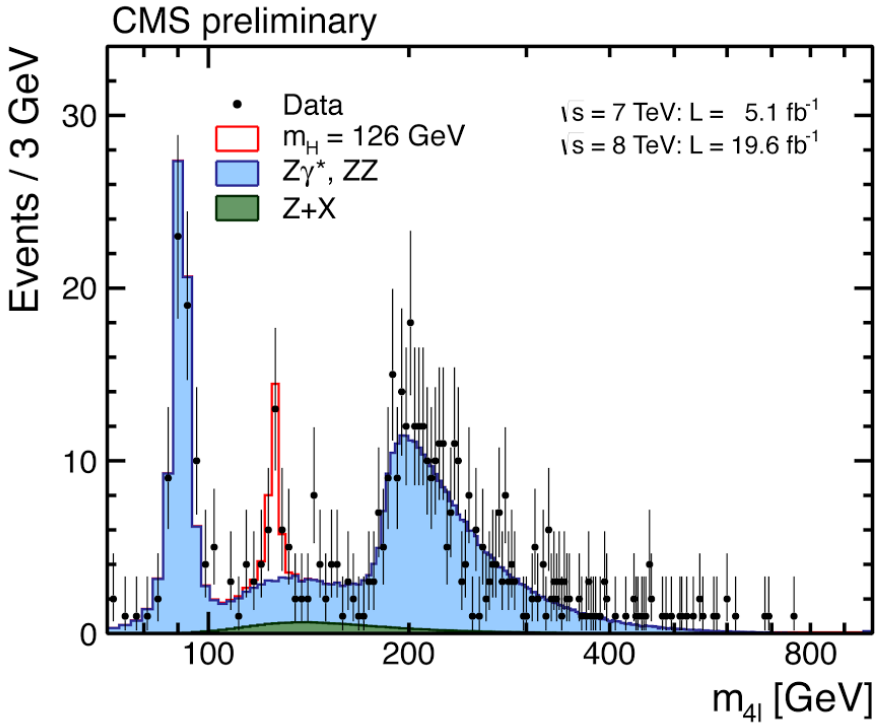

Fig. I.2. Higgs signal observed by the CMS experiment as an excess of 4 leptons events at a mass of 126 GeV (red peak) [3].

The Standard Model has done an excellent job in describing three out of the four fundamental interactions. However, the observation of matter-antimatter asymmetry, the non vanishing neutrino mass and the relatively low mass of the Higgs boson suggest that the Standard Model is incomplete. Theories proposed to expand the Standard Model include the Supersymmetric Models, some of which predict Higgs decay into neutralinos which further decay to dark neutralinos and a dark photon. While the dark neutralinos are expected to be stable, the dark photon could decay with short enough lifetime. If they decay to muons, the combined Higgs boson decay chain has a spectacular experimental signature with four muons and a missing (invisible) momentum due to undetected neutralinos [6]. An illustration of such process is shown in Fig. I.3.

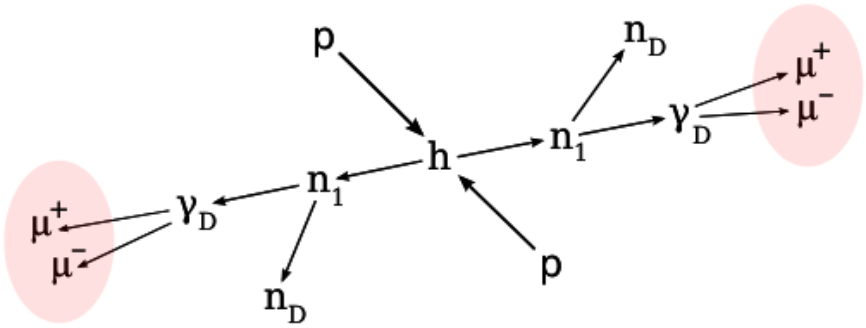

Fig. I.3. An example of a possible decay of a Higgs boson in the context of super symmetry with hidden sectors into pairs of invisible neutralinos n_d and a dark photon γ_d, subsequently decaying to pairs of muons.

The dark particles produced by the Higgs boson can travel some distance before decaying. We usually refer to that distance in terms of their proper lifetime τ so that the average distance traveled by a dark photon in its own frame can be expressed as cτ. Other possible processes include the Higgs decaying into heavy dark Z bosons, Z_D, which can decay to muon pairs, i.e.:

$$pp \rightarrow H \rightarrow Z_D Z_D \rightarrow \mu^- \mu^+ \mu^- \mu^+.$$

The example physics process discussed here is only one example of several well motivated theoretical models predicting existence of new long-lived particles, which could be produced at the LHC and discovered by the CMS and ATLAS experiments. If realized in Nature, these models could explain the origin of dark matter, neutrino mixing and mass, as well as the baryon asymmetry in the Universe.

The Large Hadron Collider (LHC) is an international project oriented to the discovery of theories beyond the Standard Model. The heart of the LHC is the accelerator, a ring of 27 km of circumference that's used to accelerate Hadrons up to relativistic speeds. At energies measured at the center of mass in the order of 14 TeV and intensities in excess of of 10^{34} cm^{-2}s^{-1}, the particle beams travel in opposite directions inside the ring until they collide, 40 million times per second, in specifically designed points where the beams are directed to cross each other.

There are seven detectors located at these crossing points. Two of the largest experiments, the Compact Muon Solenoid (CMS) and A Toroidal LHC ApparatuS (ATLAS), are general purpose detectors, while ALICE (A Large Ion Collider Experiment) and LHCb (LHC-beauty) are smaller experiments designed for specific studies. LHCf (LHC-forward), Moedal (Monopole and Exotics Detector at the LHC) and Totem (Total Cross Section, Elastic Scattering and Diffraction Dissociation) are oriented to measure specific properties of the residual particles after the collisions. The general view of the LHC and the detectors can be found in Fig. I.4. Search for the Higgs boson, tests of the Standard Model and searches for new physics signatures motivated the construction of the biggest particle accelerator in the world.

After the first run of the LHC in 2012, the collider went to a long shutdown period after which it is planned to restart in 2015. The center of mass energy is expected to increase to 13 - 14 TeV and the luminosity up to 10^{34} cm^{-2}s^{-1}. These upgrades are the first ones in a list of planned improvements scheduled for the LHC. The upgrades are necessary in order to increase the amount of

data available for analysis, allowing for a better understanding of Higgs sector and possible new discoveries.

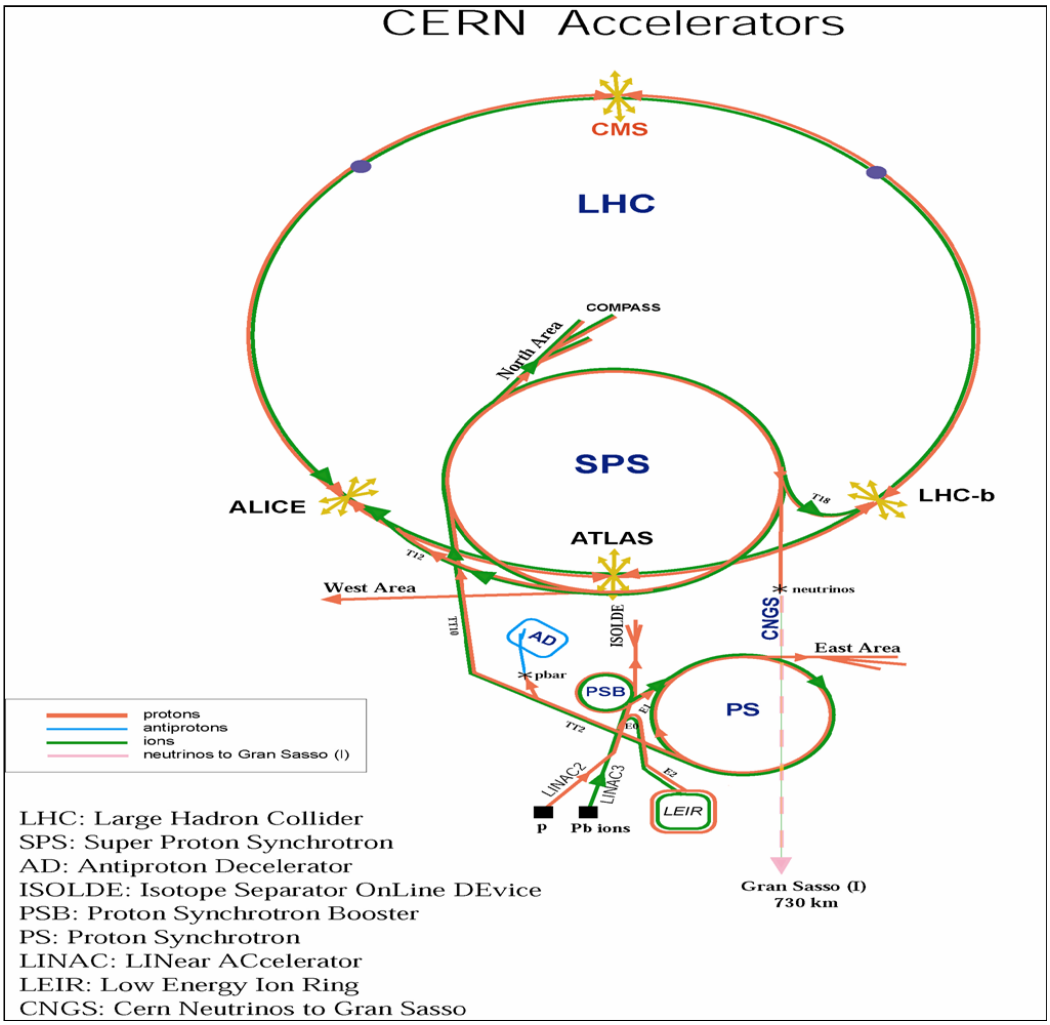

Fig. I.4. Large Hadron Collider (LHC) at CERN [4].

The Compact Muon Solenoid (CMS) detector is a general purpose particle detector designed for precision measurements of the products coming from proton proton collision. The core of the detector is a solenoid whose 3.8 T magnetic field bends charged particles as they fly inside the detector hitting multiple layers of detection. As it can be seen in Fig. I.5, the innermost layers are reserved for the silicon tracker that detects charged particles and registers their momentum.

After the tracker, the electromagnetic and hadron calorimeters stop most of the charged particles and measure their energy. The magnetic solenoid is placed around the calorimeters and provides a constant magnetic field. The muon spectrometer is placed at the outermost layer in the detector because muons can nearly freely pass through significant amount of matter.

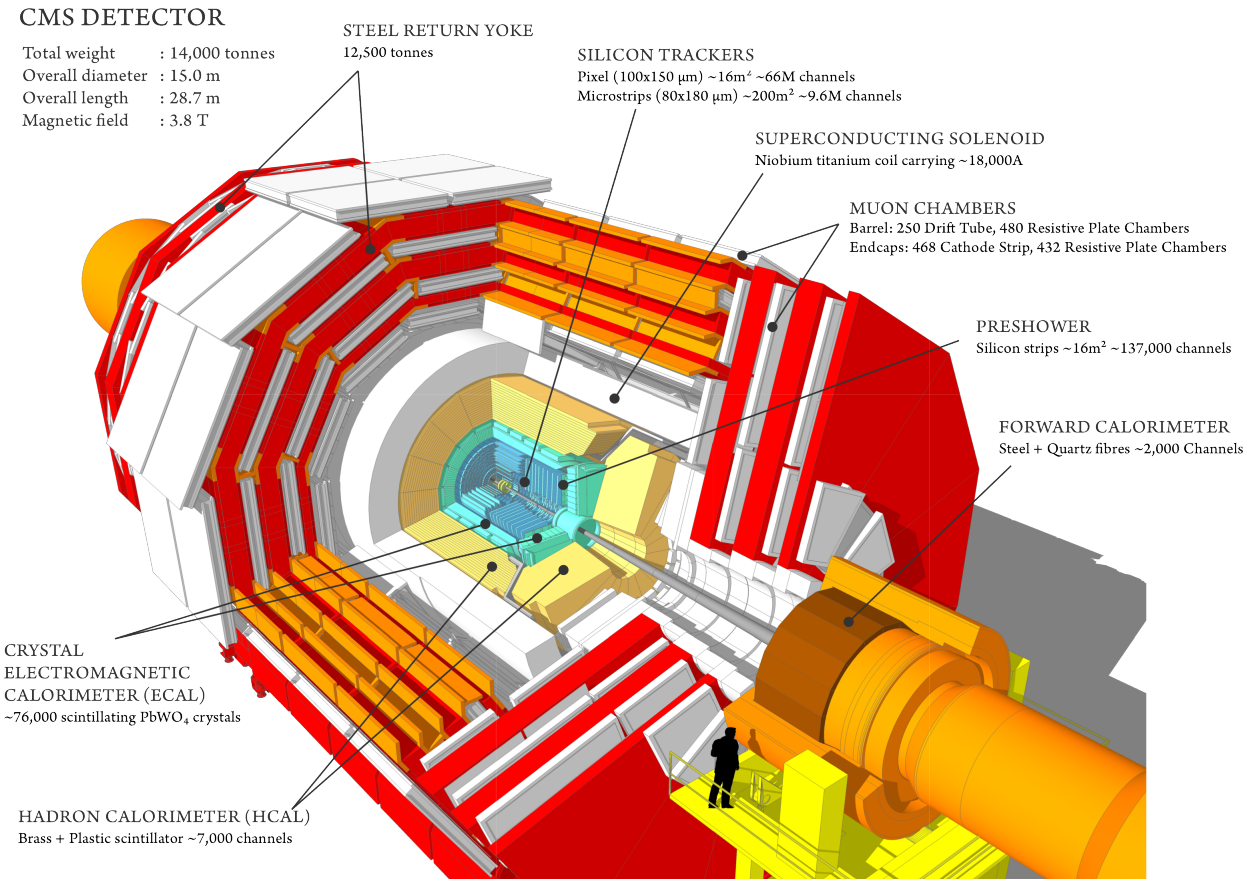

Fig. I.5. Overall disposition of the CMS experiment showing the different layers of detection. The black silhouette of a man is for comparison of the size [5].

The CMS registers information from the silicon tracker, the eletromagnetic and hadron calorimeters and the muon system in order to reconstruct the collision events at the crossing point. An illustration of event reconstruction is shown in Fig. I.6 displaying a candidate event possibly com-

ing from a Higgs decay into a pair of photons.

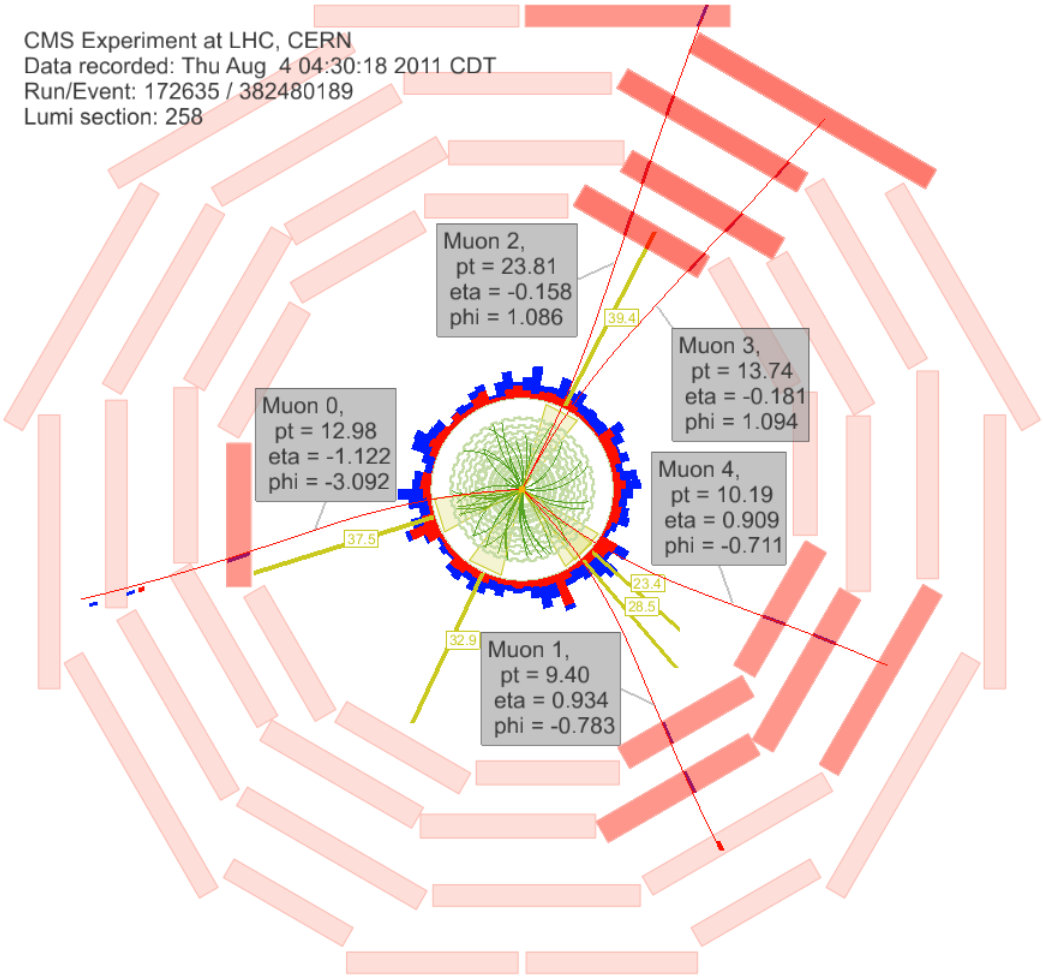

Fig. I.6. Example of an event reconstruction using the DT muon system (light red) in the barrel region of the CMS detector as well as the calorimeters (red and blue towers) and the silicon tracker (green tracks). If the event satisfies the triggering requirement, the information is stored [6].

The muon system is a cylindrical shaped arrangement of detection chambers surrounded by a return yoke for the magnetic field. It is composed of the barrel and endcap regions. The barrel region relies on the Drift Tubes (DT) detector while the endcaps use Cathode Strip Chambers (CSC) sys-

tem for track measurements. Both regions also use Resistive Plate Chambers (RPC) to assist with triggering. Future upgrades include the addition of Gas Electron Multiplier (GEM) chambers in the endcap and overall faster electronics for the whole CMS detector [4, 7].

At high luminosity, the information generated by the CMS detector system adds up to 2 MB per collision event. At a rate of 40 million collisions per second the amount of information adds up to 76 TB of data per second. That is enough information to stack a 50 m pile of Blu-ray discs every single second. Moreover, most of that information does not represent any new or interesting physics discoveries and can be discarded safely. The trigger system is designed to perform an ultra-fast selection of potentially interesting data to diminish the rate of data to the level at which the data can be written to disk for offline analysis, reducing the number of events from 40 million to just hundreds of events per second. This is done at a incredible speed by recognizing events that carry potentially interesting new physics, for example requiring high energy muons as well as information from the tracker and calorimeters. The energy can be measured by reconstructing the transverse momentum of a particle, which is the momentum perpendicular to the beam line (refer to Section II.1), and applying selections to get rid of non interesting events.

As it was shown in Fig I.2, some models beyond the Standard Model predict decays of the Higgs particle into neutral particles that travel a small distance before decaying into muons. High energy particles are often a requirement for an event to be classified as interesting. As it will be shown, displaced muons are most likely to be discarded in the current trigger configuration. Therefore, the upgrades on the trigger system should account for the increase rate of particles and for detection of displaced muons that could lead to new physics discoveries.

In this thesis we will describe the CMS muon system as well as the current triggering algorithm implementation and its shortcomings. At the end we propose an algorithm that can solve the limitations of the current trigger system and which can be implemented as part of the CMS muon

trigger upgrades for the ultra high luminosity running.

Chapter II discusses the CMS muon detector in more detail. Chapter III contains the description of the current Level 1 Drift Tube local trigger configuration. Chapter IV is a description of the Drift Tube Track Finder algorithm. In Chapter V, we discuss the shortcomings of the current DT Track Finder and we propose a solution for it. Chapter VI contains the conclusions of this Undergraduate Scholar thesis.

CHAPTER II

MUON DETECTOR OF THE CMS EXPERIMENT AT THE LHC

The CMS detector is one of the multipurpose spectrometers in the LHC designed to reconstruct and analyze high energy proton-proton collisions. The Muon System of the CMS detector is one of the key elements of the overall system designed to be efficient and reliable in order to satisfy the requirements for muon detection in search of new physics phenomena. In this chapter we will describe the muon system in more detail.

II.1 CMS Coordinates System

As it was shown in Fig. I.5, the shape of the CMS detector is best described using cylindrical coordinates. Fig. II.1 is a longitudinal view of the detector showing the main radial ($\hat{r}$) and $\hat{z}$ axis. The azimuth angle ϕ is perpendicular to the plane of the Fig. II.1 and can be defined using Fig. II.2. The polar angle θ is defined to measure the particle's direction in the r-z plane.

The polar angle θ is not a Lorentz invariant with respect to the boost along the z-axis. A better alternative is the pseudorapidity, η, defined as follows:

$$\eta = -\ln\left\{\tan\frac{\theta}{2}\right\}.$$

The use of the pseudorapidity as a spatial coordinate comes from its relationship with the longitudinal momentum, p_L, given by:

$$\eta = \frac{1}{2}\ln\frac{\mid \mathbf{p} \mid + p_L}{\mid \mathbf{p} \mid - p_L} = \tanh^{-1}\frac{p_L}{\mid \mathbf{p} \mid}.$$

The coverage of η and θ can be found in Fig. II.1, which also shows the general layout of the CMS muon system and its two major parts: the barrel and the endcap regions. The barrel sector

is divided into five wheels (Wheel: -2, -1, 0, 1, 2) and four stations (MB: 1, 2, 3, 4). The endcap region is also divided into four stations (ME: 1, 2, 3, 4) and two rings (Ring 1 and 2). Stations ME1 include an extra ring to maximize precision close to the beamline.

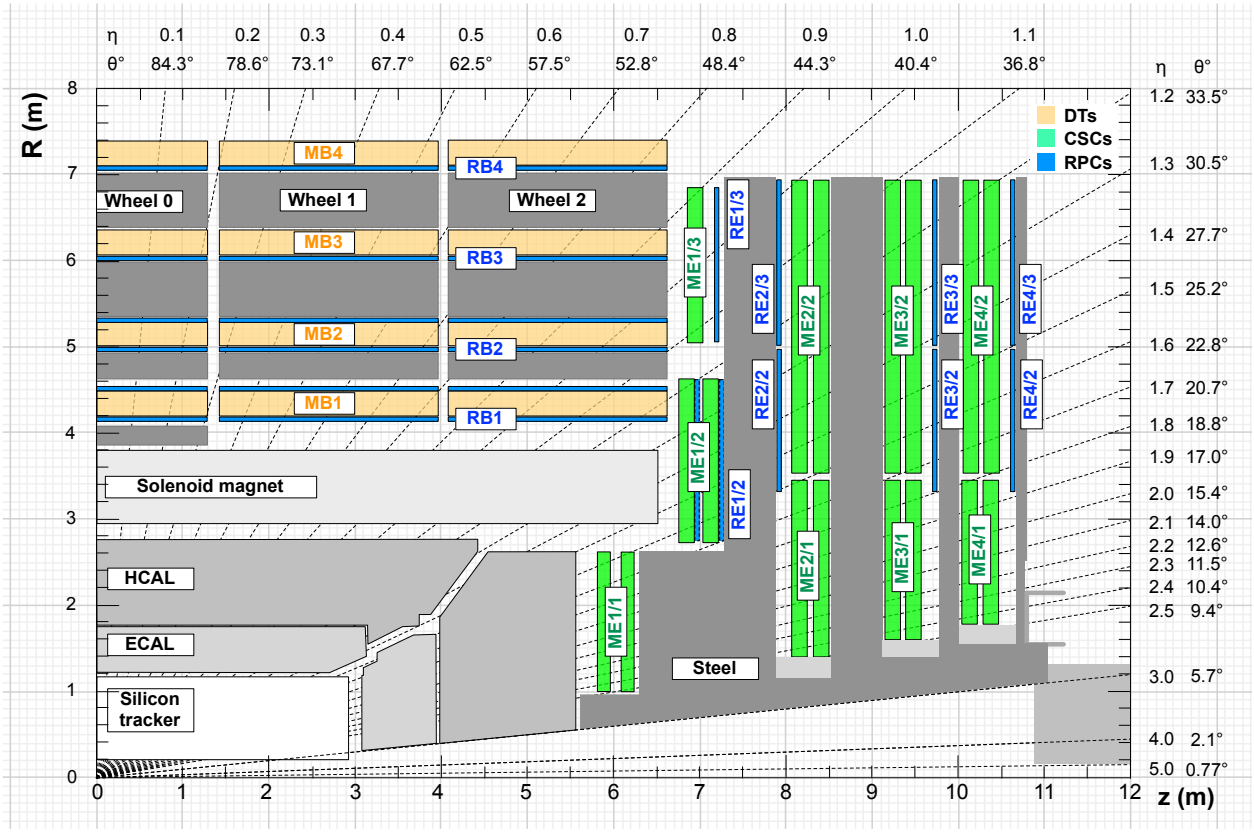

Fig. II.1. Longitudinal view of the CMS detector illustrating the positive η coverage of the Muon System. The barrel region covers the region $-1.1 \leq \eta \leq 1.1$ (light orange chambers), while the endcap region covers the eta region $\mid \eta \mid \geq 0.9$ (green chambers). Since this view measures the positions r and z, the plane is often called the r-z plane (η view) [9].

Fig. II.2 defines the ϕ coordinate measured in the global position of the CMS detector. It ranges from 0° to 360°.

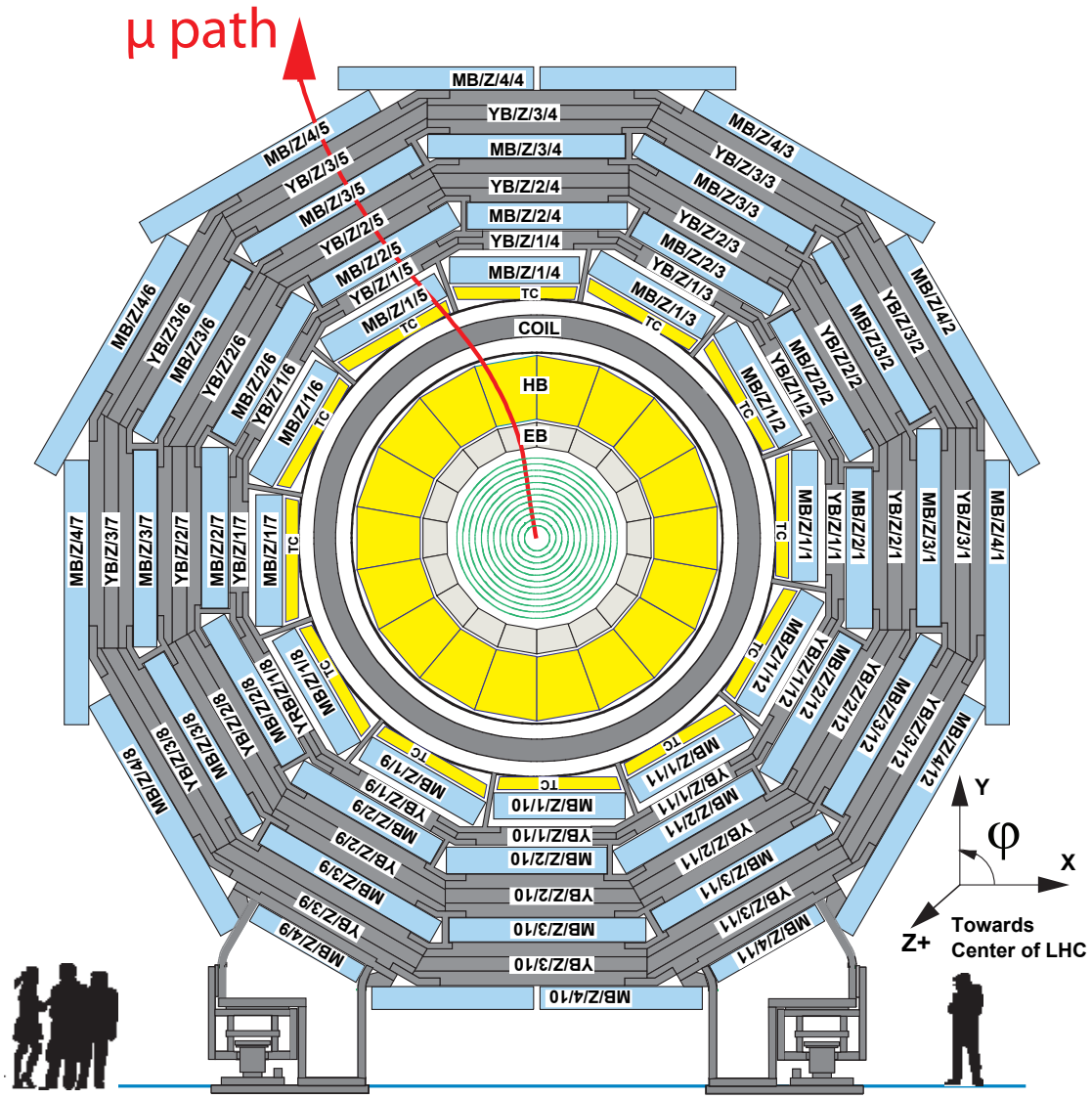

Fig. II.2. Transverse view of CMS barrel region. The four barrel muon stations (MB/Z/X for X = 1,2,3,4 stations) display their coverage range and individual position inside the muon system. The position coordinate ϕ is measured from the $\hat{x}$ axis while the radial component (r) is measured from the center of the detector. That is why this plane is also called the r-ϕ plane (ϕ view) [9].

Three coordinates are needed to specify any point in the CMS detector's global system of coordinates. They can be combinations of $\boldsymbol{r}_\perp, \boldsymbol{z}, \boldsymbol{\phi}$ as in cylindrical coordinates, but often $\boldsymbol{r}_\perp, \boldsymbol{\eta}, \boldsymbol{\phi}$ are used for simplicity (η is related to the polar angle θ, while $r_\perp$ is the radial component in cylindrical coordinates). These coordinates can be related to the $\hat{x}, \hat{y}, \hat{z}$ global coordinate system.

The magnetic field points in the $\hat{z}$ direction and it is almost constant to 3.8 T inside the solenoid. The force acting on a charged particle is given by the Lorentz force:

$$\boldsymbol{F} = q\frac{\boldsymbol{p}}{m} \times \boldsymbol{B}.$$

The cross product from the magnetic contribution to the Lorentz force, $\boldsymbol{p} \times \boldsymbol{B}$, can also be written as $p_\perp \cdot B$, with $p_\perp$ the perpendicular component of the momentum with respect to the magnetic field. Since the magnetic field points in the $\hat{z}$ direction, $p_\perp$ is actually perpendicular to the beamline and it is called the transverse momentum, p_T. In other words, the magnetic bending of the trajectory of a charged particle is proportional to the transverse momentum p_T in the configuration of the CMS experiment.

At any r position away from the beamline, one can define the *bending angle* that the trajectory makes with the radial direction. This bending angle ϕ_B is related to the transverse momentum p_T of the particle. The higher the p_T of a particle, the less it bends in the magnetic field. As muons traverse further away from the center of the detector and through the layers of the muon system, the return field bends a muon trajectory backwards. The muon system of the CMS detector has a resolution of $\Delta\phi$ of about to 0.005 mrad in the ϕ coordinate with the purpose of reconstructing the transverse momentum as precise as possible.

II.2 CMS Muon Detectors

The muon system consists of four muon stations interleaved with the steel return yoke allowing the possibility for an independent momentum measurement outside the coil. The existence of several muon stations ensures the reliability and redundancy of the system. As it is shown in Fig. II.1, the CMS muon system is divided into two parts: the endcap region, which is located at the edges of the detector, and the barrel region, a cylindrical-like shape in the middle region. The disposition can be found in Fig. I.5 and Fig. II.1.

The barrel muon detector has 240 chambers built using Drift Tubes arranged in four concentric stations MB1, MB2, MB3 and MB4. It is divided into five wheels (Fig. II.1) of twelve sectors (MB 1/1/X for X=1,2,...,12 sectors) of roughly 30° in ϕ coverage each, as shown in Fig. II.2. Each sector comprises four measuring stations (MB). To avoid pointing cracks, chambers in different stations are staggered. Station MB4 is special as it has almost 100% acceptance because of the modules being installed like shingles around the outside of the detector. The only dead area is near the supporting feet. Stations MB1 and MB2 are arranged in such a way that a muon always crosses at least one of them. The arrangement of MB3 with respect to MB1 and MB2 ensures that every muon escaping the barrel crosses at least 3 stations. Every chamber contains a module of Drift Tubes plus one layer of RPCs for MB3 and MB4 and two layers of RPCs for MB1 and MB2.

A schematic layout of a DT chamber is shown in Fig. II.3. Each DT has 12 layers of contiguous drift tube cells. The layers are grouped in three "Superlayers" (SL), each one consisting of 4 staggered layers of DT cells. The innermost and outermost SLs, labeled SL1 and SL3 in the figure, are dedicated to the ϕ coordinate measurement in the CMS bending plane defined in Fig. II.2, while the central SL, labeled SL2, measures the z coordinate of a muon traversing the chamber in the r-z plane defined in Fig. II.1. The radial coordinate is measured using an extrapolation from the three superlayers. SL2 and SL3 are separated by a honeycomb spacer in order to give a better measurement resolution to the SL1 and SL3 combination. The outermost stations, named MB4,

located outside the steel return yokes of the CMS magnet, have only two SLs measuring the hit position in the r-ϕ coordinates.

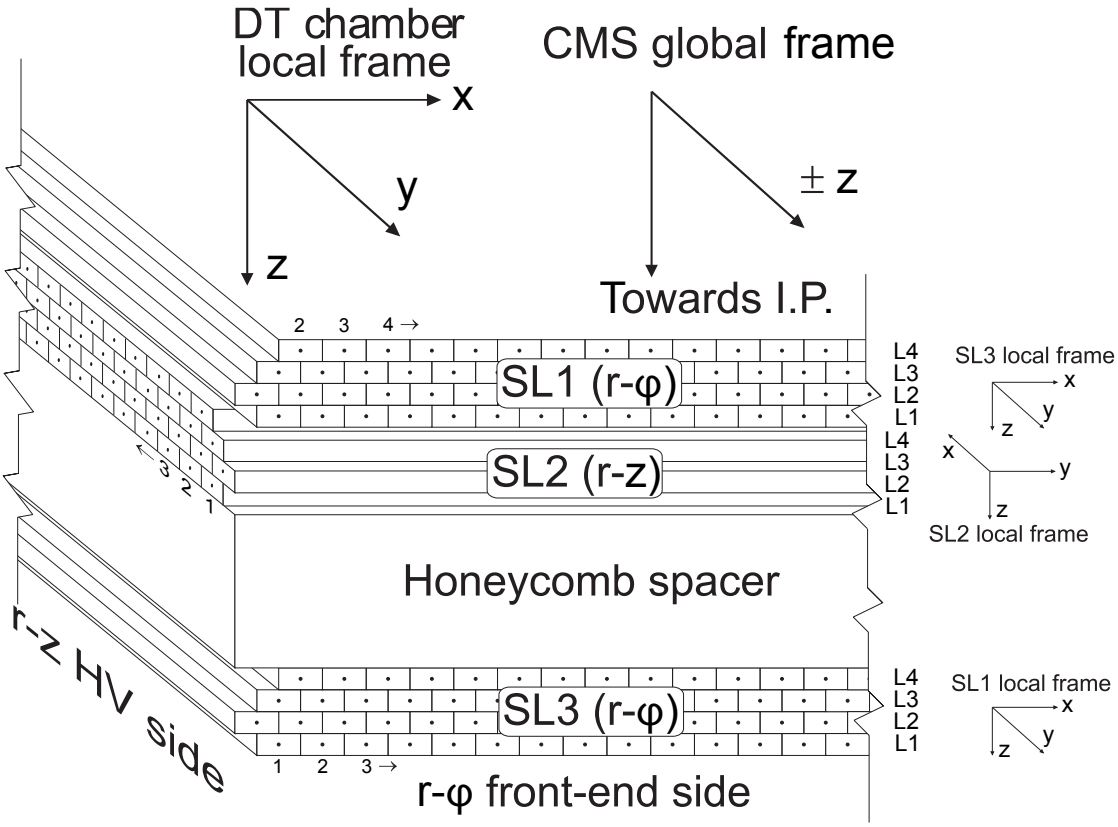

Fig. II.3. Schematic layout of a DT chamber. SL1 and SL3 are used to measure the r and ϕ coordinate in the bending plane (transverse view) of the CMS experiment (See Fig. II.2). SL2 measures the z coordinate along the the direction parallel to the beam (See Fig. II.1) [12].

The individual Drift "Tubes" are actually cells made of aluminum to ensure good mechanical precision and stiffness. The layout of a DT cells is shown in Fig II.4. The distance between the anode wires of consecutive DT cells is 4.2 cm. The cells are separated by 1 mm thick aluminum I-shaped support beams. The supports are glued between two 2.5 mm thick aluminum plates that separate consecutive layers. Aluminum strips, named "electrode strip" in the figure, are placed below and

above the anode wire of the cell to shape the electric field lines. This electric field shape guarantees a good linearity of the cell behavior over almost the entire drift volume. The chambers are operated with an Ar/CO_2 (85/15) mixture. The voltages applied to the electrodes are 3600 V for the wires, 1800 V for strips, and -1200 V for cathodes.

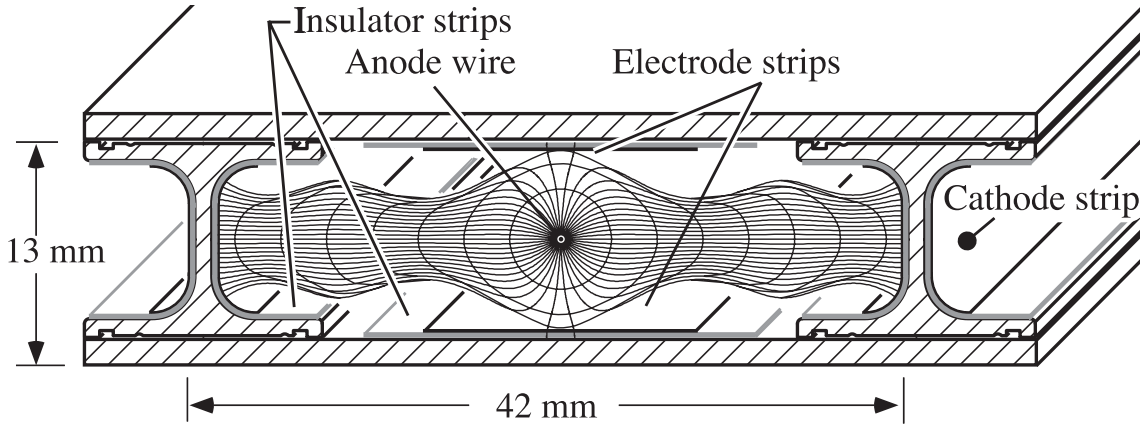

Fig. II.4. Layout of a DT cell, showing the electric field lines in the gas volume as well as the multiple components of each individual drift cell [12].

The electron drift velocity is about 54 μm/ns. The DT readout electronics is capable of recording multiple hits in the same cell, with a dead time of 150 ns between consecutive signals. At the operating value of the the magnetic field equal to 3.8 T inside the solenoid, the magnetic field in the return yoke ranges between 1.2 T and 1.8 T. Inside the active volume of each DT chamber, the residual magnetic field is generally small (below 0.2 T) so we can ignore the magnetic bending inside the DT chambers. However, MB$\pm$2 stations, due to edge effects, have a radial magnetic gradient of significant magnitude [12].

Each DT cell consists of tubes of 4 cm wide containing a stretched high voltage wire in the middle of the cell surrounded by a volume of gas. When a charged particle crosses it, it knocks out electrons from the gas that follow the electric field produced by the wire and create an avalanche of secondary ionization electrons. This creates "hits" in the adjacent cells that can be used to extrapolate the position of the muon and the bending angles of the trajectory, see Fig. II.5.

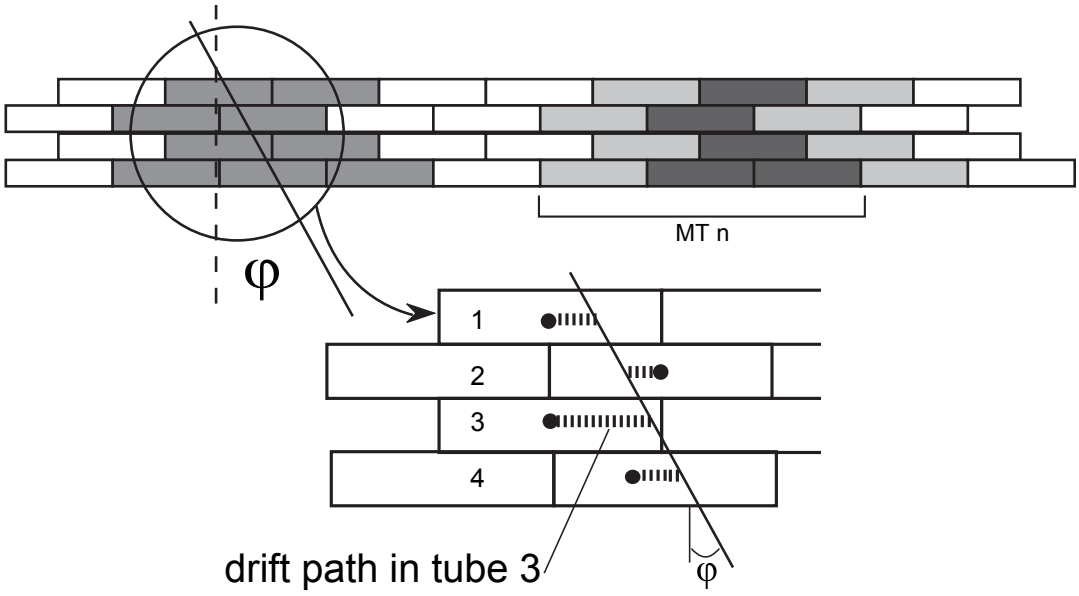

Fig. II.5. Drift Tubes basic function diagram. A muon creates electrons that are accelerated toward an anode wire inside each tube. By measuring times of the hit arrival (ionization avalanche arrival) we can reconstruct the path of the muon [9].

Because there are two superlayers dedicated to measure the ϕ coordinate, a simple extrapolation between the hits in SL1 and SL3 can be used to reconstruct the local path that the muon traveled inside the DT chamber along with the bending angle measured with respect to the local normal. This bending angle ϕ_B depends only on the tangent approximation of curvature of the entire trajectory of the muon as it was bent by the magnetic field. Since the bending depends only on the transverse momentum, the bending angle measured at the station, ϕ_B, is dependent on the transverse momentum of the particle p_T. Moreover, using the extrapolation from SL1 and SL3, it is also possible to precisely calculate the angular coordinate position ϕ of the hit with respect to the

global coordinates of the barrel muon system. The information coming from the SL2 can be used to calculate the z position of the hit and a combination of the three superlayers can be used to extrapolate the radial position (r) of the hit.

From the local reconstructed path, the global positions and the bending angles, the system is able to calculate the muon path and reconstruct the momentum of the particles traversing the detector.

II.3 CMS Muon Trigger System

The original CMS detector has been designed for a luminosity of 10^{34} cm^{-2}s^{-1} with an average of 20 overlapping collision events per beam crossing (every 25 ns or 40 million crossing per second). This input rate must be reduced down to $\sim$100 kHz, which is the maximum rate that could be archived by the online computer farm data storage. The CMS experiment has a trigger system that reduces the rates in two steps. At the first step, the Level 1 trigger (L1 Trigger) reduces the data from 40 MHz to as much as 100 kHz. It makes a deicions every 25 ns with an allowed maximun latency of 3.2 μs. The selected events are forwarded to the second step, the High Level Trigger (HLT). The HLT is a software trigger that reduces the rates from 100 kHz down to $\sim$100 Hz. The HLT has $\sim$100 ms to make a decision using more advanced tests in order to forward events considered interesting.

The Level 1 Muon Trigger decision logic is illustrated in Fig. II.6. It consists of the Drift Tubes (DT) Trigger, the Cathode Strip Chambers (CSC) Trigger and Resistive Plate Chambers (RPC) Pattern Comparator Trigger (PACT). The information is forwarded to the Global Muon Trigger where the best four muon candidates are chosen.

The good spatial precision of DT and CSC ensures a reasonably sharp momentum threshold while their multilayer structure provides for an effective background rejection. RPC detectors have supe-

rior time resolution, which ensures unambiguous bunch crossing identification. Properly combining the information from the systems results in high efficiency and powerful background rejection.

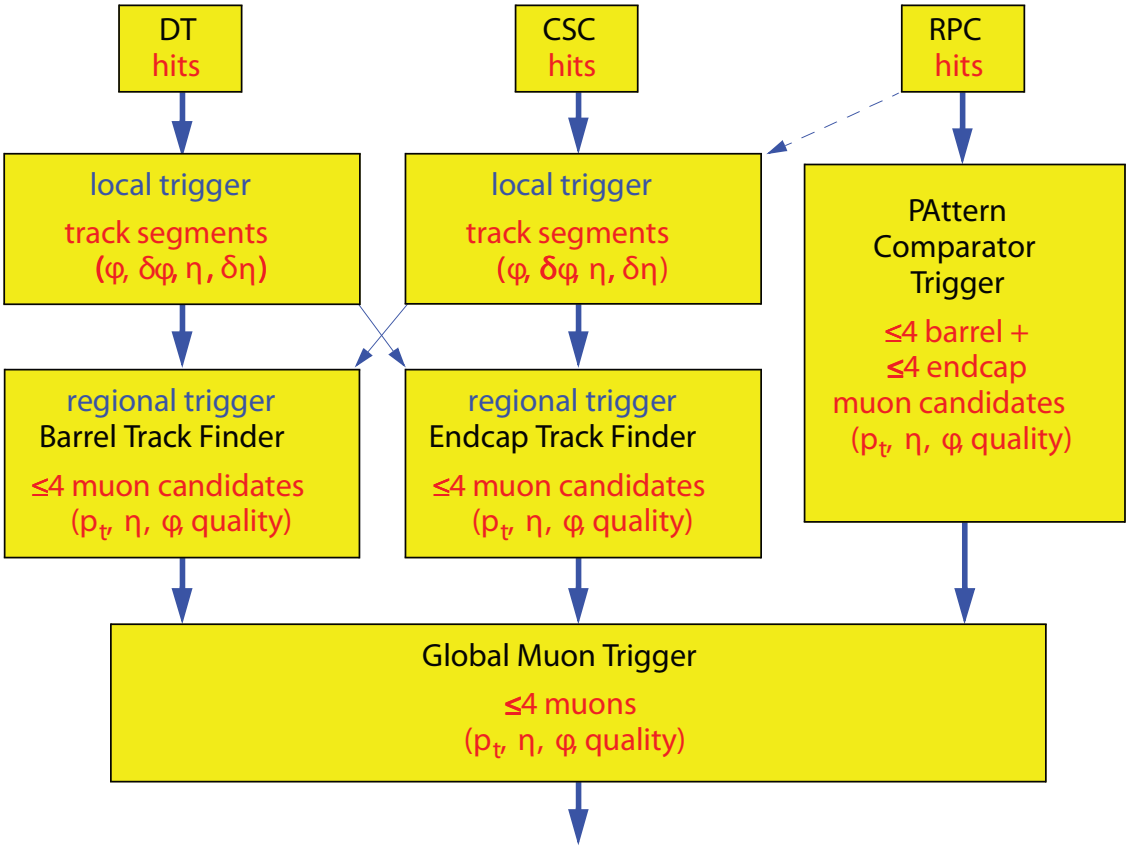

Fig. II.6. Overview of the Muon Trigger system in the CMS experiment [9].

The step-by-step reconstruction and decision structure of the Muon Trigger is shown in Fig. II.7. DT and CSC electronics first process the information from each chamber locally, therefore they are called local triggers. The local triggers measure the coordinates and bending angle of a muon, reconstruct a segment of the track and send it to the Track Finder.

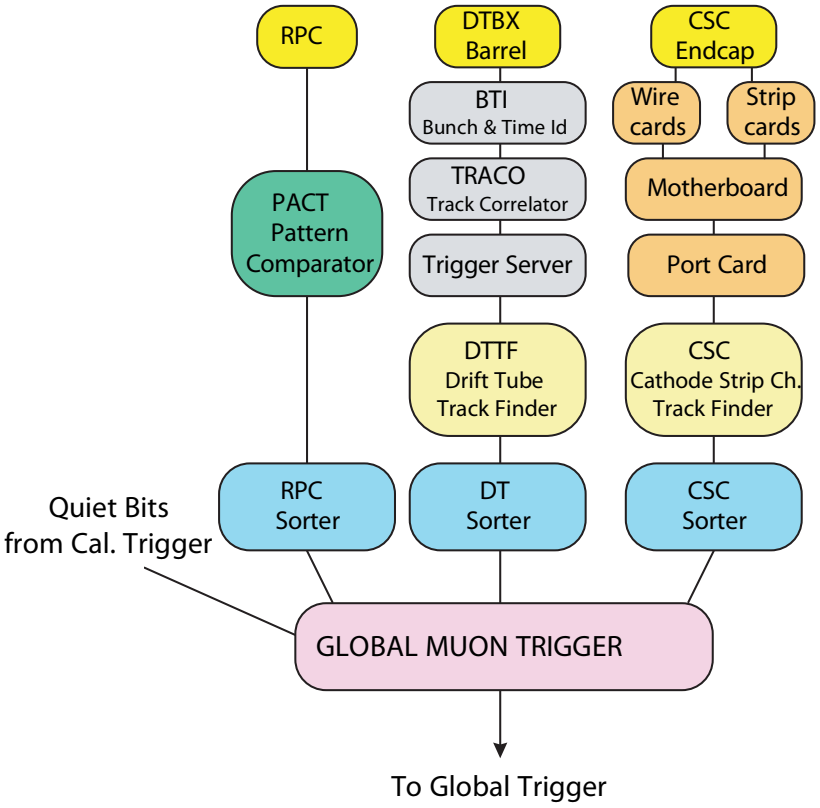

Fig. II.7. Schematic of the Muon Trigger up to the Global Trigger [9].

Data is exchanged between DT and CSC in the overlap region ($0.8 \leq \mid \eta \mid \leq 1.2$). In this way the Barrel Track Finder covers the region of $\mid \eta \mid \leq 1.0$, whereas the Endcap Track Finder covers $1.0 \leq \mid \eta \mid \leq 2.4$. This setup is planed to be updated by 2017 to combine the local trigger information of DT and CSC with RPC inputs on the regional track finders.

In the Track Finder, the local segments are combined to form a full muon track. The Track Finder also assigns the p_T of the track. Track Finder plays the role of a regional trigger. Up to 4 best (highest p_T and quality) muon candidates from each system are selected and sent to the Global Muon Trigger.

CHAPTER III

DT LOCAL TRIGGER RECONSTRUCTION

As one can see in Fig. II.7, the local DT trigger reconstruction consists of the Bunch and Track Identification (BTI), the Track Correlator (TRACO), the Trigger Server (TS) and the Sector Collector Board (SCB) steps. In this chapter, we will describe each component in more detail.

III.1 Bunch and Track Identifier

The Bunch and Track Identifier (BTI) system is directly interfaced to the front end of the DT muon chambers. The basic scheme of a BTI unit is displayed in Fig. III.1. Each BTI receives information from nine DT cells and each cell can be linked to up to three different BTI units.

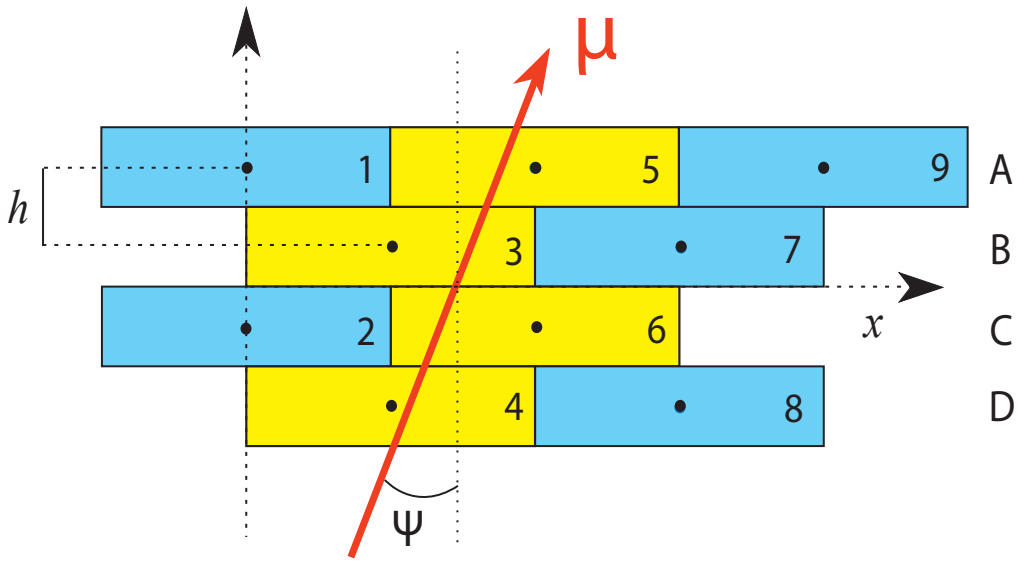

Fig. III.1. Bunch and Track Identifier (BTI) layout showing the channels allocation and important parameter.

Using the signals from the wires, the BTI generates a trigger at a fixed time after the passage of the muon. This constant time allows for a precise Bunch Crossing timing measurement. Each BTI searches for coincidences in the alignment of the hits in the four equidistant planes in each SL.

The BTI can extract the track segment information (position and direction) from the hits in the cell arrangement. The association of the hit is based on a mean time technique that uses the fact that there is a fixed relation between the drift times or any three adjacent planes.

BTI is the implementation of a trigger device based on the generalized mean timer resolution method. It works on groups of four layers of staggered drift tubes, aiming to the identification of the tracks giving signals in at least three out of the four measurement planes (ABCD). This method relies on the fact that the particle path is a straight line within the DT chamber and that the wire positions along the path (the measurement points) are equidistant to a length h.

At the superlayer level, the parameters calculated are the position and the angular *k parameter* defined as follow:

$$k = h \tan(\Psi).$$

Where Ψ is the *bending angle* of the track with respect to the normal to the chamber plane in the transverse projection and $h = 13$ mm is the distance between wire planes. The actual BTI candidate track finding algorithm computes in parallel several track patterns hypotheses. A pattern is identified by a sequence of wire numbers and labels arranged depending on the direction of the muon near the given wire. Any given pattern includes six pairs of planes (AB, BC, CD, AC, BD, AD), each one providing a measurement of the position and of the k parameter of the track.

If there is a coincidence of all six k parameters, the trigger corresponds to the alignment of four hits and it is marked as High Quality Trigger (HTRG), while in any other case, with a minimum

of three coincident k-parameters, it is due to the alignment of only three hits and it is marked Low Quality Trigger (LTRG). The angular resolution is track pattern dependent and is generally worse for LTRGs.

The impact position of the muon is not used in the track selection algorithm and it is computed only for the selected triggering pattern. Position and angular resolution depend on the drift velocity and on the sampling frequency of the device.

The spatial resolution of one BTI is better than 1.4 mm while the angular resolution is better than 60 mrad. With the present geometric parameters of the chamber the BTI equations are fully covering the angular range up to $\Psi_{MAX} = \pm 45^{\circ}$.

The quality, the k parameter and the global positions are sent to the TRACO, which associates the track segments and performs noise rejection. Indeed each BTI of the chamber outer SL is interfaced to three Track Correlators.

III.2 Track Correlator

TRACO is designed to associate portions of tracks in the same chamber relating predefined groups of BTIs among them. The TRACO interconnects the two SLs that measures the ϕ coordinate. If a correlation can be found, the TRACO defines a new track segment with better angular resolution and assigns it a quality factor.

The introduction of this device was necessary since the BTI is intrinsically a noisy device and therefore a local preselection and a quality certification of the BTI triggers is required.

The current design connects four BTIs of the inner superlayer (SL1) to twelve BTIs of the outer superlayer (SL3) allocated as shown in Fig. III.2 assuring a full coverage up to Ψ_{MAX}.

The algorithm starts selecting, among all the candidates in SL1 and the SL3 independently, the best track segment, according to preferences given to the trigger quality (High or Low Quality Trigger) and to the track proximity to the radial direction to the vertex. Then it find the best matching options for the k-paratemer. Upon a correlation between SL1 and SL3 is found, the system assigns a K_{COR} value of the matched k-parameters and X_{COR} value depending on the bending angle and the large lever arm between SL1 and SL3.

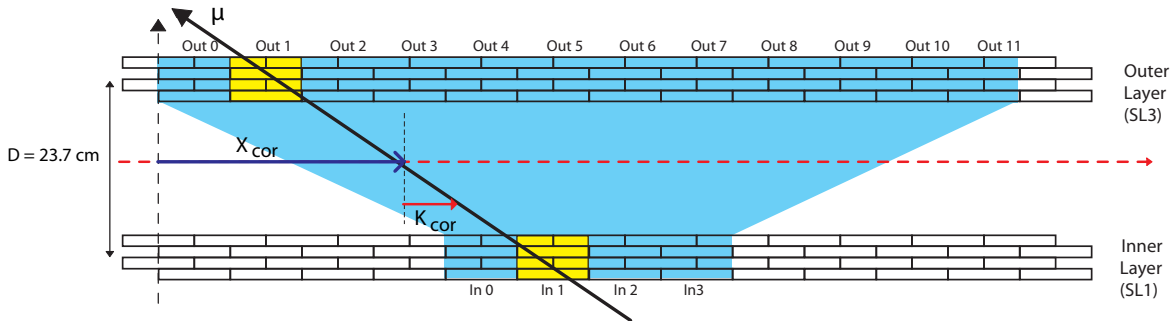

Fig. III.2. Track Corelator layout. Individual BTI in yellow are being matched. See DT chamber details in Fig. II.3.

Owing to the long lever arm between the two SLs the angular resolution of a correlated track candidate is improved, thus significantly improving the BTI precision.

These parameters are converted, using programmable look up tables, to the chamber reference system: position (X_{COR} is transformed to the coordinate angle ϕ and the K_{COR}-parameter becomes the bending angle ϕ_B). The output of the TRACO can be seen in Fig. III.3. The chosen track is forwarded to the chamber TS, for further selection.

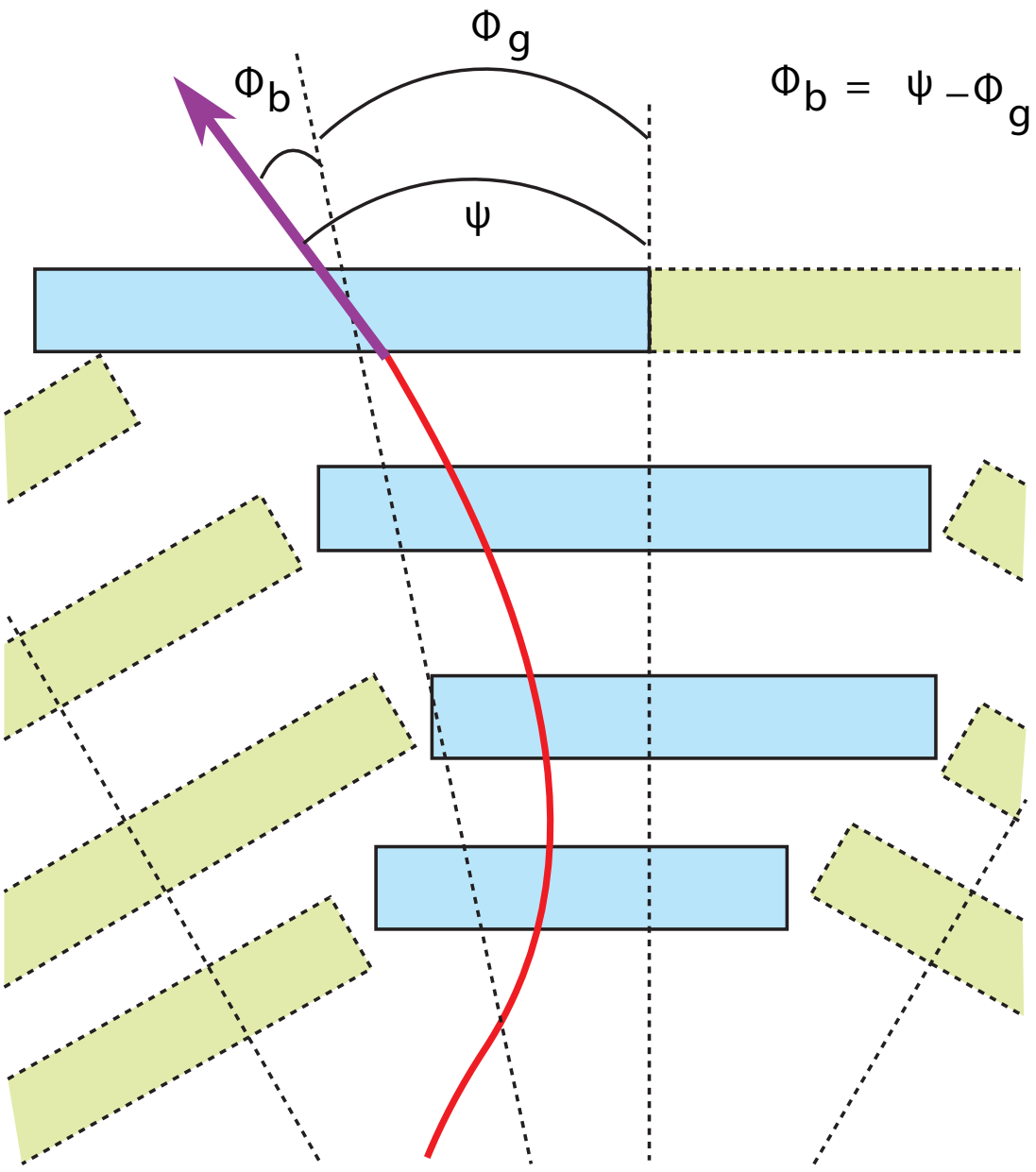

Fig. III.3. Track Corelator output parameters. The bending angle ϕ_B can be calculated at any station but it's generally larger at the first station MB1 [9]

III.3 Trigger Server

The Trigger Server selects the two best trigger candidates among the track segments selected by all TRACOs in a muon station and sends them to the Sector Collector. The TS is composed by two subsystems: one for the transverse view (TSϕ, See Fig. II.2) and the other for the longitudinal view (TSθ whose parameter can be seen in Fig. II.1). The simplified work of the TS is displayed in Fig. III.4.

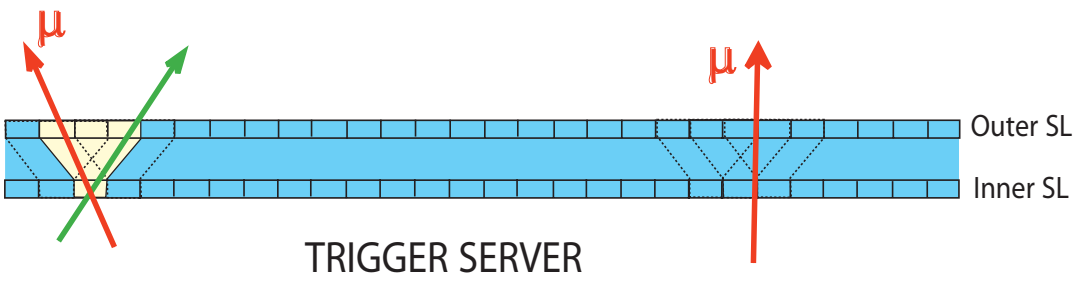

Fig. III.4. Trigger Server basic scheme. It sorts the best two muons by quality (red) while reduces the fake production caused in TRACO (green). The results are forwarded to the Sector Collector that delivers them to the Regional Muon Trigger.

TSϕ receives information from the TRACO while TSη receives the coordinate measurements directly from the BTI.

TSϕ is divided into Track Sorter Slave (TSS) and Track Sorter Master (TSM). The TSS preselects the tracks with the best quality and the smallest bending angle ϕ_B based on a reduced preview data set coming from the TRACO. A selected line in the TRACO with the best track is then activated and the TRACO sends the full data to the TSM. The corresponding preview data are also sent to the TSM for a second stage processing. The TSM analyzes up to seven previews from the TSS. The

output of the TS consists of the two tracks with the highest p_T. There is one TSM per muon station.

TSη groups the information from 64 BTIs units per chamber. From each BTI sends the trigger bit and the quality bit to the TSη whose output consists on the position of the track and an associated η quality. The output from TS is forwarded to the Sector Collector Board.

III.4 Sector Collector Board

The Sector Collector Board (SCB) is placed in the mini crate of the fourth station of each sector. This SCB acts as a readout data from each of the 30° sectors on which the barrel is divided in the ϕ view. The SCB has high speed optical links to the TS and to the Regional Muon Trigger (RMT).

The data forwarded to the Regional Muon Trigger from each muon chamber station contains the ϕ coordinate, the bending angle ϕ_B, the quality assigned by TRACO, the track and overlap parameters, the η position and η quality, and synchronization information control. This information is used in the Track Finder to finally classify muons by quality and p_T.

CHAPTER IV

DT MUON TRIGGER TRACK FINDER RECONSTRUCTION AND MOMENTUM MEASUREMENT

The task of the Drift Tube Track Finder system (DTTF) is to find muon tracks in the barrel region originating from the interaction point and to measure their transverse momentum and their location in ϕ and η coordinates (defined in Chapter II). Using the trigger primitive data delivered by the Drift Tube chamber system, the DTTF reconstructs muon candidates joining together track segments caused by the same track. After the track finding process, the DTTF system assigns a transverse momentum measurement p_T, a ϕ and η coordinate measurement and a quality word to the muon track candidates. Finally, the Track Finder system selects the four highest transverse momentum tracks in the detector barrel and forwards them to the Global Muon Trigger system. The performance of the DTTF system is directly related to the performance of the Muon Chambers and to the relative alignment of the chambers in the Muon Detector system.

The main input data stream of the DTTF system are the track segments coming from the Drift Tube Trigger Sector Collector units. The Drift Tube trigger system sends one track segment in each bunch crossing. The ϕ-track segments are composed of the ϕ position, the ϕ_B bending angle, the quality, a second track segment tag to tell if there's any and calibration and suppression information used to eliminate fake track alignment in DTTF. The η-track segment data is sent through the Sector Collector as a vector hit map of the η stations containing the η and z coordinates and the η-quality. The radial coordinate is extrapolated from both η and ϕ views.

The DT Track Finder algorithm can be described as a three step process as shown in Fig. IV.1: the Extrapolation Unit, the Track Assembler and the Assignment Unit.

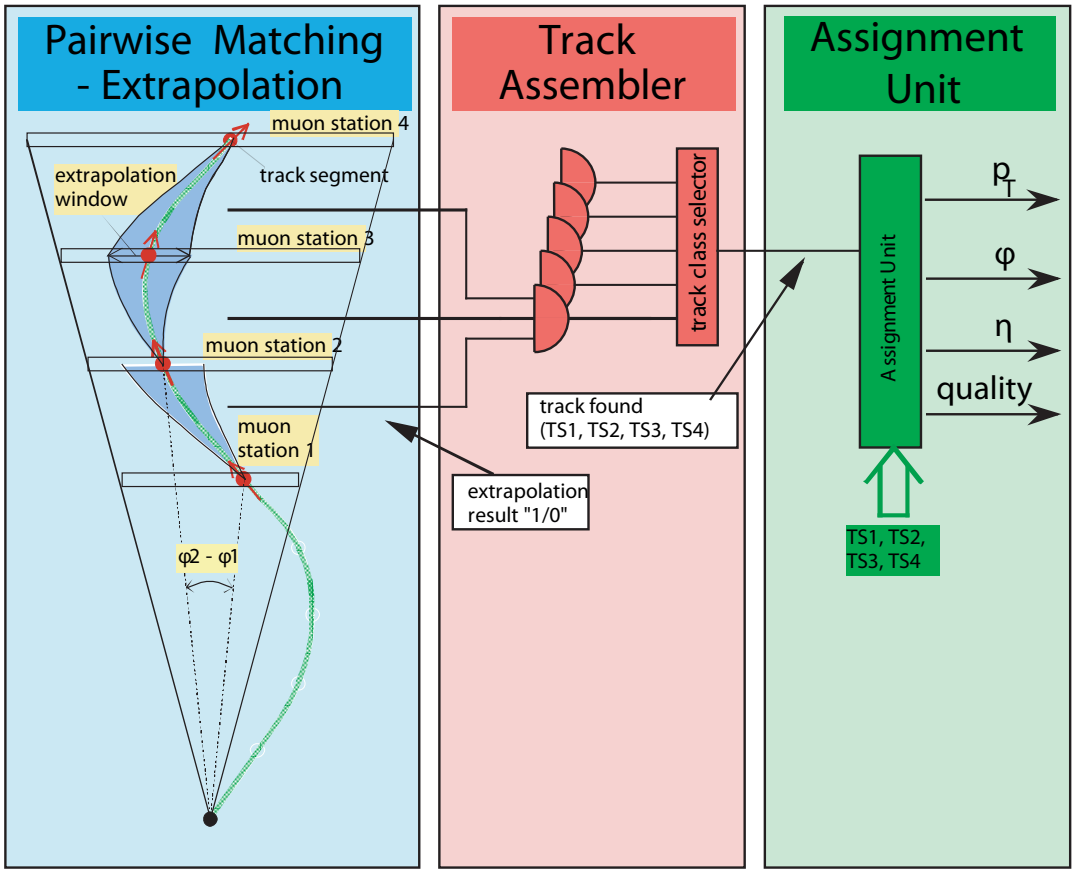

Fig. IV.1. Three step scheme of the track finder algorithm of the DT trigger system. The pairwise matching algorithm on the left. The Track Assembler in the middle and the Assignment Unit on the right [9].

IV.1 The Extrapolation Unit

In the first step the Extrapolation Unit (EU) of the Sector Processor tries to match track segment pairs of distinct muon stations, using a pairwise matching method. This is performed by extrapolating to the next station from a track segment using the spatial and angular measurement ϕ and ϕ_B of the track segment (see Fig. IV.2). The matched pairs are then forwarded to the Track Assembler Unit which links the segment pairs to full tracks. The Assignment Unit performs the last step, assigning the track parameters to the candidates.

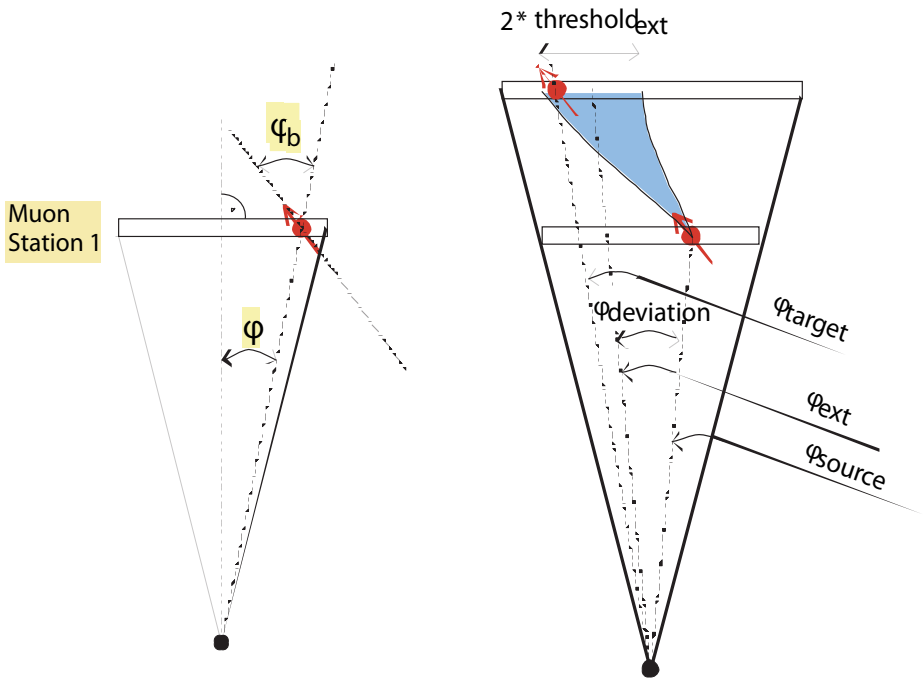

Fig. IV.2. On the left a track segment consisting on the spatial coordinate ϕ and the bending angle ϕ_B. On the right the basic concept of the pairwise matching is shown. If a track sement is found to be within the extrapolation windows given by ϕ_{ext} and threshold tt_{ext}, the extrapolation is marked as successful [9].

The basic principle of the EU is to attempt to match together track segments caused by the same track. This is done by using a pairwise matching based on the principle of extrapolation. Using the spatial coordinates ϕ_{source} and the angular measurement $\phi_{B,source}$ of the source track segment, an extrapolated hit coordinate ϕ_{ext} in another chamber may be calculated, according to:

$$\phi_{ext} = \phi_{source} + \phi_{deviation}(\phi_{B,source}).$$

The $\phi_{deviation}$ is given in terms of the bending angle of the source track segment. If a target track segment is found to be at the extrapolated coordinate within a certain extrapolation threshold tt_{ext} the match is considered done.

IV.2 The Track Assembler Unit

The task of the track assembler is to find the two tracks in a sector exhibiting the highest number of matching track segments. It selects the two highest ranking tracks from all the formed ones and outputs the relative addresses of the matching track segments. The Track Segment Router extracts the corresponding track segment data from the data pipeline using the relative addresses of the track segments. In order to reduce the number of Input/Output connections from the EUs to the Track Linker unit, only the EUs belonging to a single Sector Processor and the EUs in the next wheel neighbour Sector Processor are connected to the Track Linker unit.

The Track Linker finds tracks by setting up conditions for their existence. For instance a 1-2-3-4 track can be built, if there is an existing 1-2 extrapolation, from its target in the Muon Station MB2 there is another existing 2-3 extrapolation, and from its target in Station MB3 there is an existing 3-4 extrapolation. For the existence of the 1-2-3-4 track the target of the 3-4 extrapolation has no importance, the track extends to the Station MB4 if there is at least one existing 3-4 extrapolation. Thus this target needs no further check.

Tracks that are formed using more than two track segments requires check for the validity of the intermediate extrapolations. This means that, for the existence of a 1-2-3 track not only valid EU12 and EU23 extrapolations are needed, but also a valid EU13 extrapolation. Furthermore, the algorithm checks whether the last segment of extrapolation EU13 is the target segment of the previous EU23 extrapolation. This condition increases the protection against noise and δ rays in case of longer tracks. In Fig. IV.3 it is shown how an extrapolation from MB1 to MB2 (EU12) can be joined to an extrapolation from MB2 to MB3 (EU23) if they share the same track segment in MB2. In order to validate this joining, it is required also that an extrapolation EU13 exists, sharing the same track segment of the previous joined ones. A track consisting of three track segments is now formed.

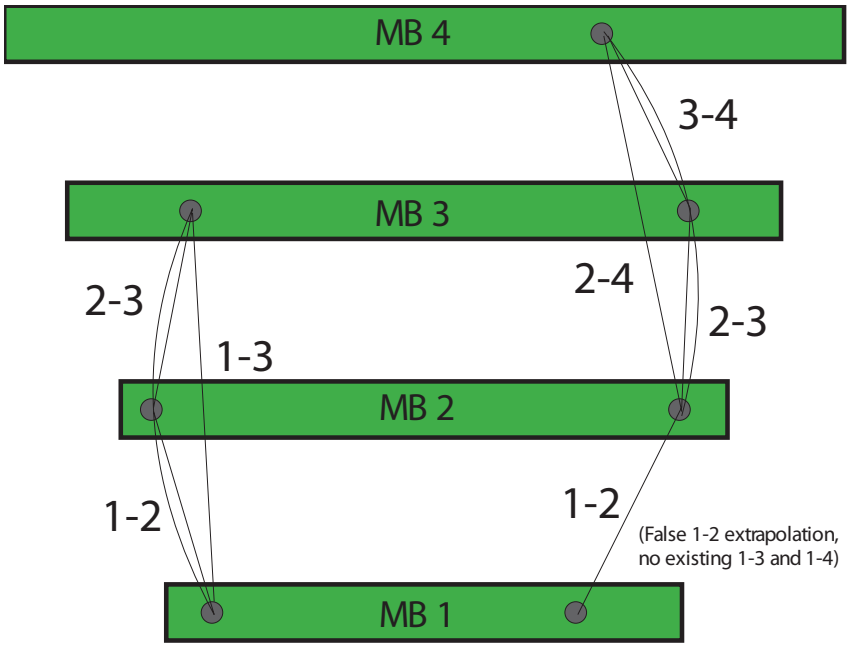

Fig. IV.3. Track Linker Algorithm. Two pairs of tracks are joined if the last track segment of the first pair is the starting segment of the second pair [9].

IV.3 Assignment Unit (AU)

The track segment addresses forwarded by the Track Linker are used to extract the physical parameters of the track segments from the data pipeline. Once the track segment data are available to the Assignment Units, memory based look up tables are used to determine the transverse momenta of the particles. The momentum and the location of the tracks as well as a quality information about the track finding is output to the GMT.

The ϕ Assignment Unit: The assigned ϕ coordinate values correspond to the spatial coordinate of the track segment in the second muon station. If the track candidates do not have a track segment in the second muon station, an extrapolation towards the second muon station position is performed, using memory based look up tables.

The η Assignment Unit: The η parameter is assigned by a specifically designed board in the η view. Since particles don't magnetically bend in the η direction, the value of η is independent of the station at which it is measured.

The Quality Assignment Unit: The quality code is assigned for each track based on the class and the previous quality numbers sent to the DTTF. Track classes are ordered according to number of participating track segments and to the momentum resolution, which is better when assigned using the inner muon station track segments.

The p_T Assignment Unit: The transverse momentum (p_T) is assigned using the difference in the spatial coordinate ϕ of the two innermost track segments. Fig. IV.4 shows the difference in the measured azimuthal position (ϕ) as a function of the transverse momentum. For some station pairing the relationship between the difference in ϕ coordinates and the transverse momentum is not unique. This is due to low p_T particles which are back bent in the transverse plane. In such cases the difference in ϕ coordinates tends to be as low as in the case of high-momentum particle.

The *bending angle* ϕ_B of the innermost station track segment can still distinguish between low momentum and high momentum particles. The relationship is parametrized using two sets of functions, one set for low transverse momentum track candidates and one set for high transverse momentum track candidates. The bending angle of the *innermost station track segment* (usually in MB1) selects which function has to be used in the transverse momentum assignment. Memory based look up tables are actually used in the hardware for the transverse momentum assignment, parametrizing the two sets of functions. The charge of the particle is assigned using the ϕ_B sign of the *innermost track segment* used to reconstruct the candidate, i.e. checking the most significant bit of the track segment ϕ_B data.

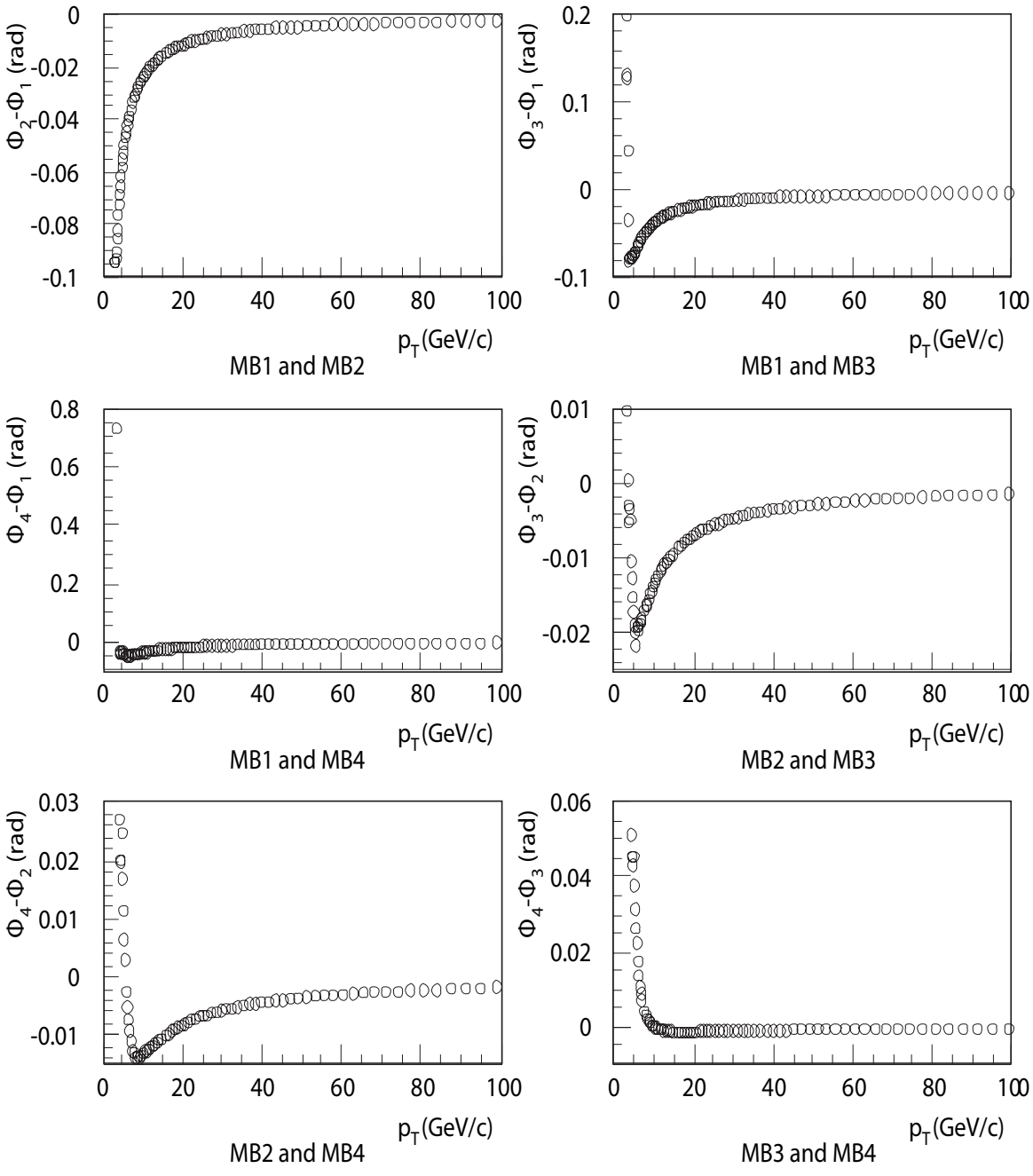

Fig. IV.4. Differences in the azimutal coordinate ϕ as a function of the momentum p_T for all muon station paring [9].

The calculation of the p_T values happens using the difference of the input track segment ϕ values in those two stations having the lowest number, as shown in Fig. IV.5. This way there are separate look up tables (LUTs) used for 1-2, 1-3, 1-4, 2-3, 2-4 and 3-4 station pairs. In order to solve the problems caused by the ϕ difference (p_T ambiguities), the p_T assignment uses different LUTs for high p_T and low p_T cases. The value of the ϕ_B determines which LUT will be used.

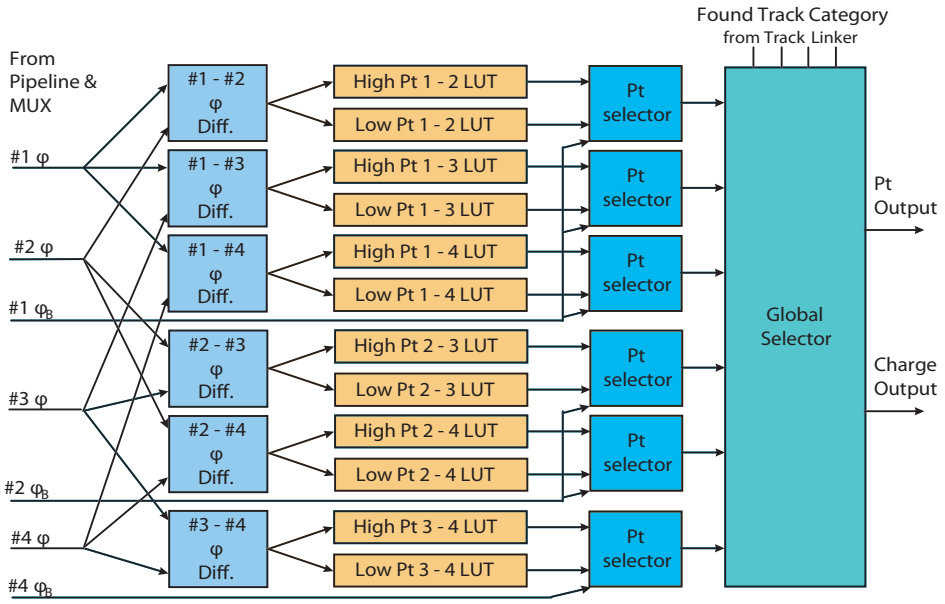

Fig. IV.5. p_T Assignment Sub Unit scheme in the AU logic. The p_T is calculated using the angular position difference between stations (ie.: $\phi_{MB2} - \phi_{MB1}$) while the bending angle ϕ_B dictates which LUT will be selected [9].

The values of p_T with respect to the bending angles ϕ_B and azimutal positions are pre calculated in LUTs stored in memory for faster calculation without adding any latency. The values of p_T, ϕ_B, quality and the position coordinates ϕ, η, z, r are forwarded to the Global Muon Trigger.

CHAPTER V

STUB ALIGNMENT ALGORITHM FOR THE UPGRADED CMS MUON TRIGGER

In this chapter, we will show that the current implementation of the trigger is inefficient for muons coming from particles with displaced vertexes, and we propose an algorithm that is capable of reconstructing and correctly assigning momentum for muons independent of whether they are prompt or displaced.

For the purpose of this study, unless otherwise noted, only magnetic field and material effects are taken into account in the simulation. The possible path of muons is estimated using Geant4 [15] with detailed CMS geometry defined. The CMS detector sensitive material response as well as electronics response and resolution are not taken into account. This choice of a perfect detector response is justified by the most salient features of the muon trigger performance being driven by the material and magnetic field effects. Full detector electronics response simulation will be needed to study finer details of the muon trigger algorithm performance for displaced muons.

As a benchmark, we selected a scenario illustrated in Fig. I.3 with Z dark boson (Z_D) mass of 20 GeV and proper life time cτ of 1000 mm and use the track impact parameter, $|d_{xy}|$, to evaluate the muon trigger algorithm performance for displaced muons.

The track impact parameter is defined as the closest distance between the extrapolated trajectory track and the interaction point. Fig. V.1 illustrates the definition of track impact parameter in the transverse view of the CMS barrel muon system. The track impact parameter is one measure of the displacement of dark particles before decaying into pairs of muons whose track is reconstructed in the DT muon system. The resulting track impact parameter $|d_{xy}|$ distribution for the selected benchmark configuration is shown in Fig. V.2.

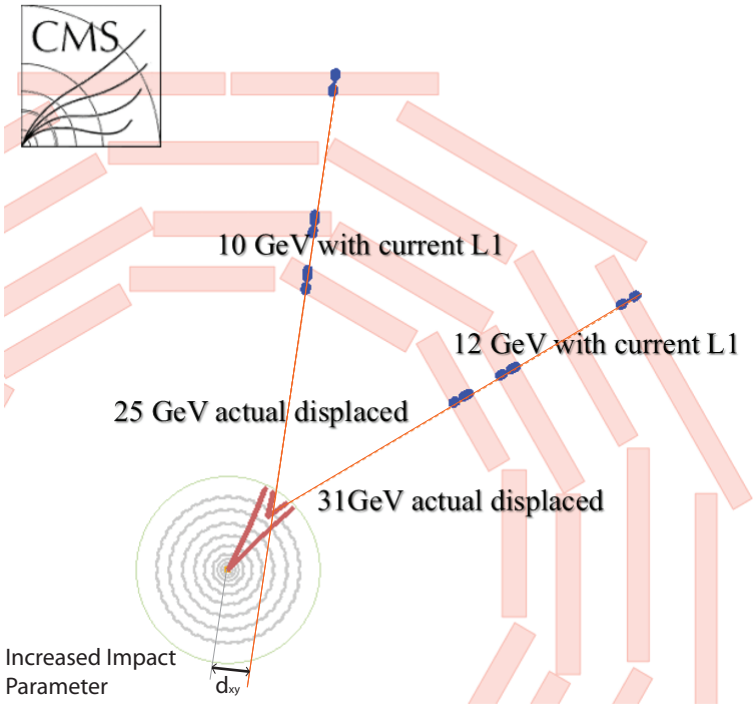

Fig. V.1. Transverse track impact parameter $|d_{xy}|$ definition.

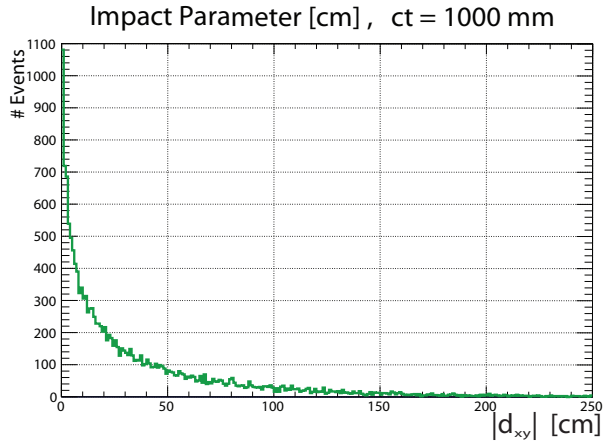

Fig. V.2. Impact parameter measured at MB01 for muons with 2 GeV $\leq p_T \leq$ 60 GeV, coming from displaced vertexes of Z_D decays, where Z_D have a mass of 20 GeV and cτ of 1000 mm.

V.1 Shortcoming of the Current Implementation

The current configuration for the stand alone DT trigger has done an excellent job at reconstructing the p_T of the particles coming from the interaction point. As it can been in Fig. V.3 the approximation of the p_T using the bending angle works very well for prompt muons. Note the general agreement of this distribution with that in Fig. IV.4. This reaffirms the choice of using perfect detector response simulation to evaluate performance of the muon trigger algorithms.

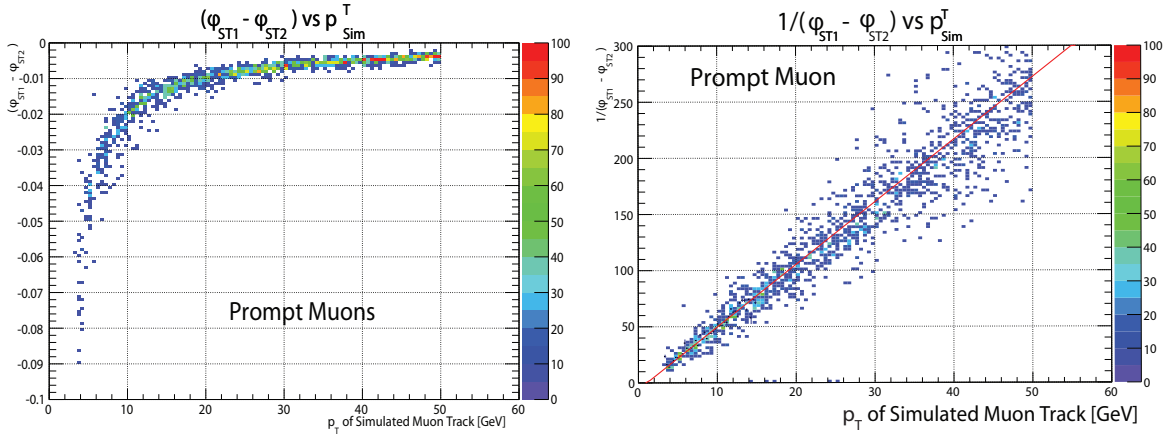

Fig. V.3. $\phi_{ST1} - \phi_{ST2}$ vs p_T for prompt muons measured at MB01 suggested an inverse relationship (Left). Plot of $1/(\phi_{ST1} - \phi_{ST2})$ vs p_T for prompt muons showing a lineal relationship. The Transverse Momentum (p_T) can be reconstructed from this angle difference $\Delta\phi_{ST1-ST2}$ (Right).

Typical trigger selections targeting final states with muons, require presence of one or more sufficiently energetic muon candidates and (optionally) other objects, such as electrons or jets. Muon transverse momentum p_T is the usual figure of merit determining how energetic a muon is, that is why the output of the Muon Trigger System pays especial attention at the reconstruction of the p_T. Maintaining high selection efficiency for interesting events implies maintaining sufficiently low p_T thresholds, while maintaining high rejection of background (non-interesting) events. If an interesting physics event is not triggered on, it cannot be analyzed as the data is lost forever. The increase in the luminosity of the HL-LHC results in very large increases in the rates of events re-

quiring more efficient and elaborate methods to increase background rejection while maintaining acceptable thresholds.

Muon+Track Trigger:

One effective solution for the high rate problem planned to be implemented at CMS is design of a new tracker trigger capable of precision measurement of momenta of charged tracks. Combining muon and tracker information at the trigger level eliminates mismeasurements of the momenta performed using muon spectrometry data alone, allowing large reduction in the trigger rate without losses in efficiency as it can be seen in Fig. V.4.

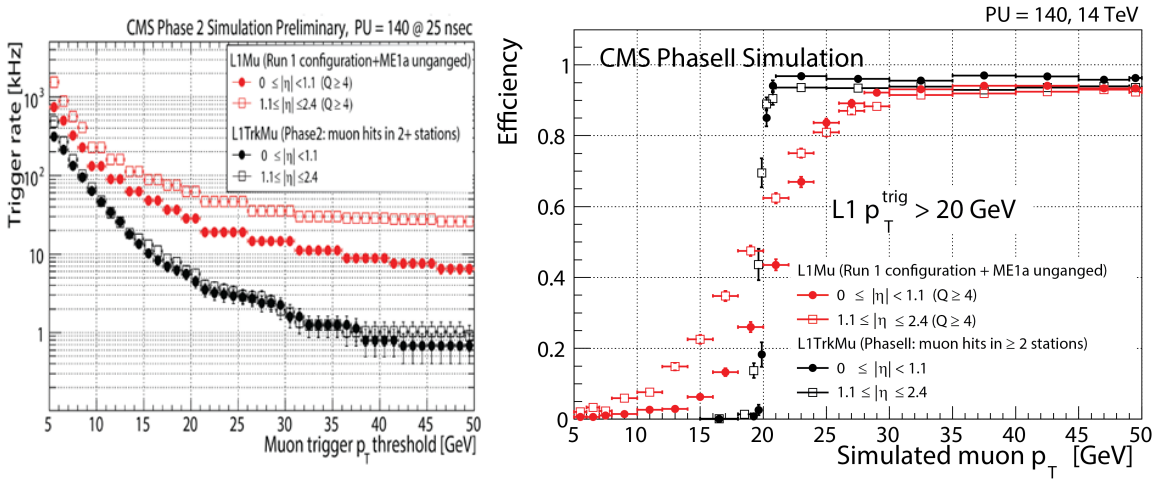

Fig. V.4. Addition of tracking allows very large reductions in L1 trigger rate for standard electron and muon triggers (left). Turn on curves for the DT stand alone (red) and Track + Muon trigger (black) configurations (right) [16].

As Fig. V.4 (right) suggeststs, this solution of combining the Muon System with the inner tracker is very efficient at detecting muons coming from the collision point (interaction point). Fig. V.4 (left) shows that the background rejection is dramatically improved by adding the track to the stand alone muon system.

However, Muon + Track Trigger is very inefficient for detecting events with even the slightest displacement. Fig. V.5 (left) shows that as the impact parameter increases, the reconstruction efficiency for the Track + Muon quickly drops to zero. The blue curve of Fig. V.5 suggests that standalone muon trigger can still reconstruct such events.

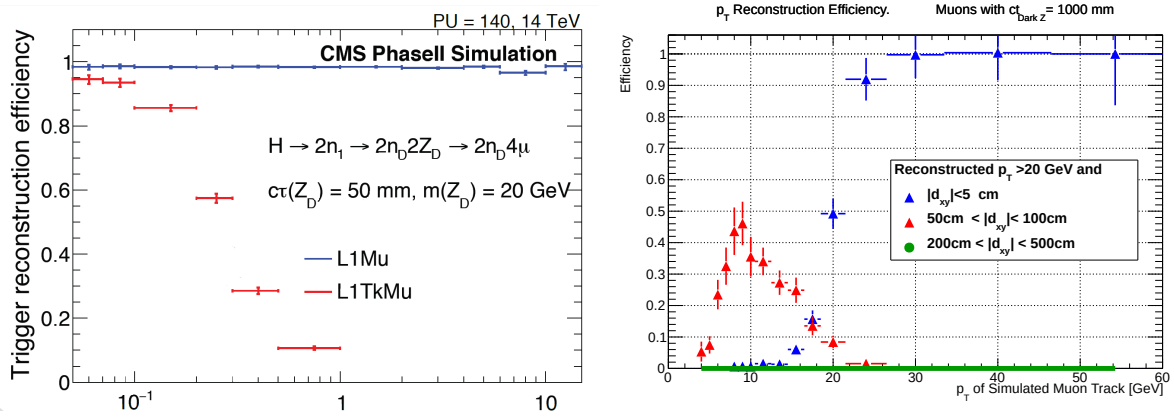

Fig. V.5. Tracking trigger efficiency vanishes for muons with even moderate impact parameters $|d_{xy}| \geq 3$ mm. Standalone muon trigger is capable to reconstruct such muons (left) [16]. Selection efficiency for a trigger configuration requiring reconstructed $p_T \geq 20$ GeV for muons with varied degrees of displacement. Standalone Level-1 trigger muon momentum measurement does not correctly measure momentum for displaced muons. Once a p_T threshold is applied, efficiency losses quickly become dramatic with the increasing impact parameter, $|d_{xy}|$ (right).

Without sufficiently high thresholds, the currently used standalone muon trigger system develops way too high triggering rate at the increased luminosity of the LHC. Moreover, the current muon p_T assignment algorithm significantly underestimates p_T for displaced muons. Once L1 thresholds are applied, potentially interesting events are all but eliminated. Fig. V.5 (Right) shows the problem: A minimum requirement of $p_T \geq 20$ GeV, the efficiency of the detection of muons drops to zero as the track impact parameter increases. The current configuration will most likely discard interesting events that could potentially have insights for new physics.

The problem can be explained using Fig. V.6. A long lived dark particle decays far from the interaction point produces muons that have intrinsic large bending angles ϕ_B. The BTI station will assign a low k-factor due to this enlarged ϕ_B. Since the maximum bending angle with respect to the normal that the BTI can detect is limited by hardware constrains to $\Psi_{MAX} = \pm 45°$, a limit in the maximum bending angle measurement is imposed.

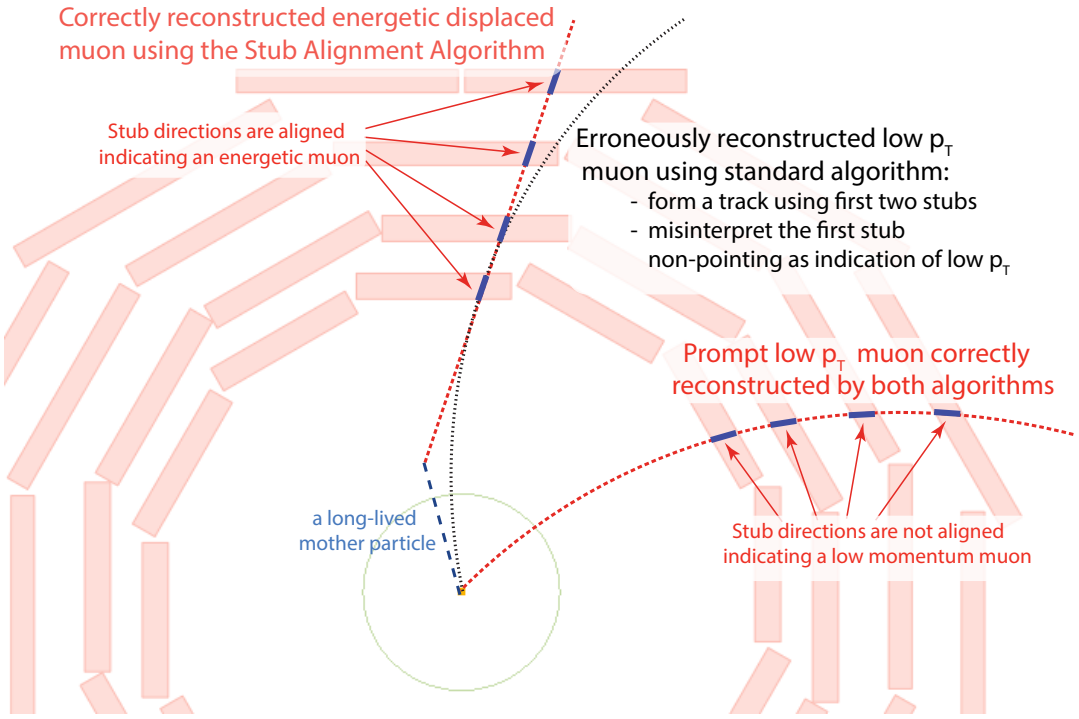

Fig. V.6. High p_T displaced muon travels along (almost) straight line and leaves track segments in DT stations. Current L1 trigger algorithm assumes the muon comes from interaction point and mistakenly assigns low momentum (curving trajectory). High energy particles are most likely to provide data for new physics, and high p_T thresholds (above 20 GeV) are applied to cope with available bandwidth. Therefore under the current trigger configuration, most of the displaced muons will be rejected.

TRACO correlates the values of the segments and assigns an angular position to the reconstructed candidate track. Because of the large value of the k-factor produced in the BTI, TRACO will also assign a large k_{COR}-factor and therefore, a low quality. A displaced muon bending angle resembles that generated by low momentum muon (See. Fig V.6). The ϕ coordinate measurement will be improved in TRACO but the bending angle will be still very large.

TS will forward the information to the DTTF, where the differences in the ϕ coordinate between the innermost stations (MB1 and MB2 ideally) will be used to reconstruct the momentum of the particle. Because of the track similarities to low p_T muons track, the system will erroneously assign a lower p_T value. Moreover, since the ϕ_B is very large, the p_T assignment unit will chose the low p_T LUT for reconstruction, leading to a even lower value in the p_T measurement of displaced muons.

Using the traditional difference in the ϕ coordinate in the standalone muon trigger will yield a significant p_T mismeasurement for displaced muons as shown in Fig. V.7. Fig. V.5 also showed that the p_T reconstruction gets worse as the impact parameter increases.

In summary, there are two problems with the p_T assignment algorithm: first, the ϕ coordinate of muons coming from displaced vertices will resemble the characteristic trajectory of low p_T muons. Second, the bending angle ϕ_B will be inherently large for displaced muons. As a result, the DTTF will most of the time use the low p_T LUT to assign the p_T using a very large $\Delta\phi$ coordinate values, leading to a much lower p_T assignment than the muon actually has. After applying a minimum p_T threshold in order to keep the rates low, the trigger system will most likely discard the displaced muons, even if they were very energetic.

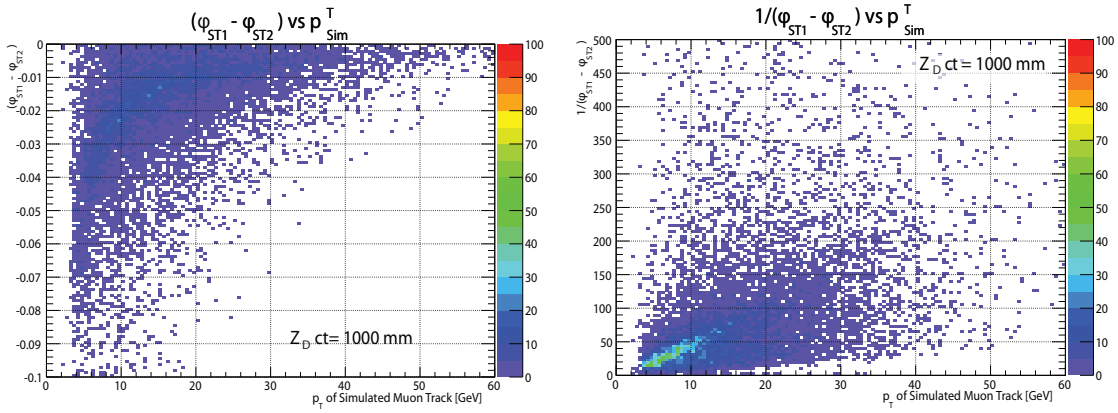

Fig. V.7. Plot of $(\phi_{ST1} - \phi_{ST2})$ vs p_T for muons coming from Z_D decays, where Z_D has a mass of 20 GeV and cτ of 1000 mm (Left). Plot of $1/(\phi_{ST1} - \phi_{ST2})$ vs p_T. The transverse momentum (p_T) cannot be appropriately reconstructed (Right)).

V.2 Stub Alignment Algorithm Description

The current algorithm relies on the difference in the ϕ coordinate to reconstruct the momentum. However, as it was shown in the previous section, this variable $\Delta\phi$ cannot reconstruct the momentum of displaced muons. The algorithm needs a new variable that is independent on the displacement of the muon to reconstruct the p_T.

Referring to Fig. V.6, a high p_T displaced muon will produce hits whose ϕ coordinates in the first two stations will resemble a low p_T prompt muon. The system will be unable to differentiate a high p_T displaced muon from a low p_T prompt muon track.

However, since high p_T muons bend very slightly as they travel through the magnetic field of the CMS detector, the variations in the bending angles measured at different stations of the DT system should remain small, even if the actual bending angle ϕ_B of the track is significant. Using this property, we can define the difference in bending angles measured at different stations, $\Delta\phi_B$, as

the new variable to reconstruct the p_T of the muon. Fig. V.8 shows the definition of the proposed variable, $\Delta\phi_B$.

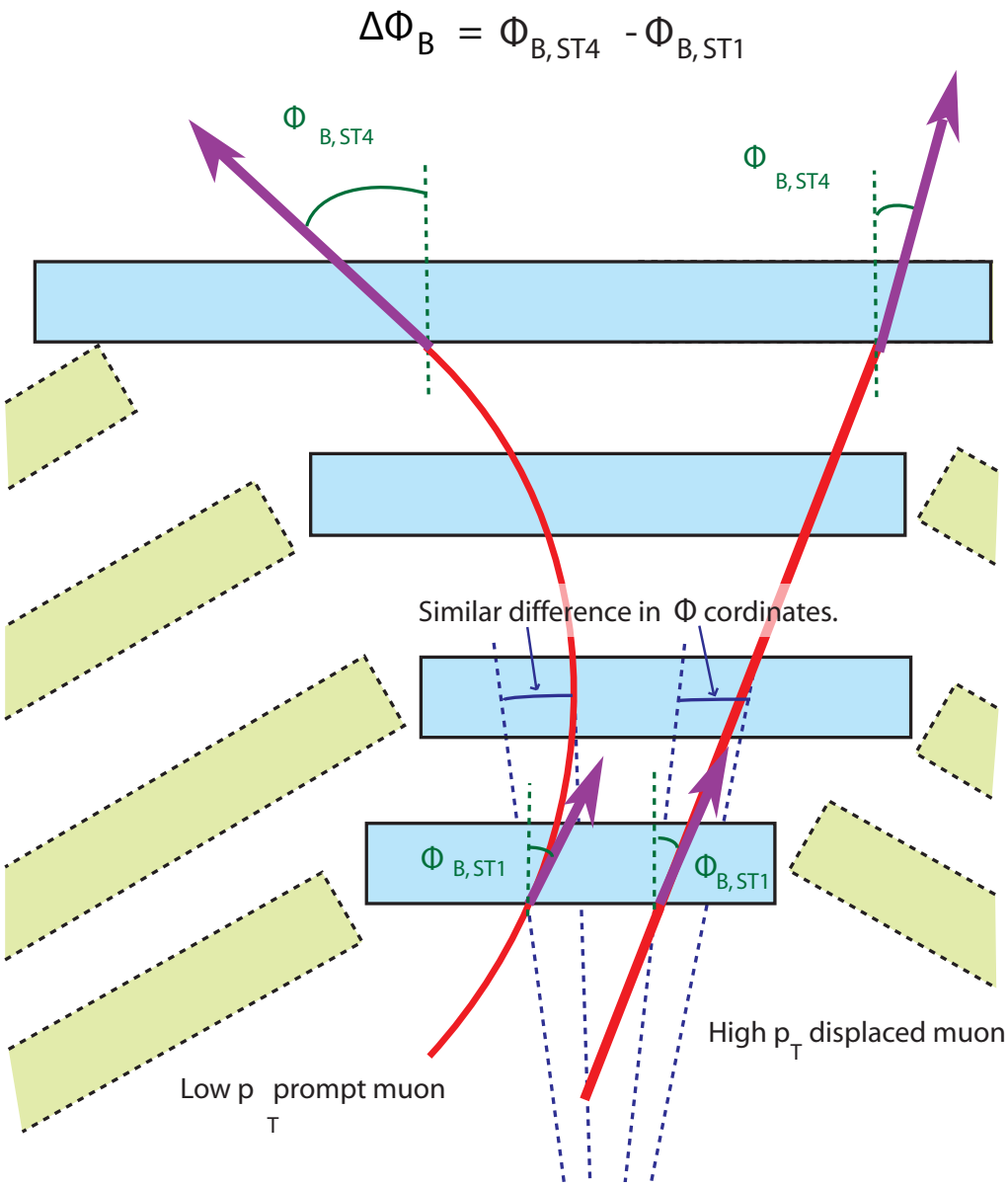

Fig. V.8. Illustration of the proposed algorithm definition for the bending angle difference $\Delta\phi_B$ between stations in the ϕ view.

Fig. V.8 shows a displaced muon and a prompt muon with almost the same bending angle at the first station $\phi_{B,ST1}$ and similar differences in ϕ coordinates. The current algorithm is unable to distinguish between them.

Even in the differences in ϕ coordinates, $\Delta\phi$, of the muons, measured at the first and second stations are the same, the bending angles differences measured at different stations, $\Delta\phi_B$, are different. $\Delta\phi_B$ remains small for high p_T muons while low p_T muons will have a large $\Delta\phi_B$. Using $\Delta\phi_B$ one can distinguish low p_T from high p_T muons.

Moreover, since we do not consider the ϕ coordinate of the muon, even if a high p_T displaced muon's track resembles the one from a low p_T prompt muon in the r-ϕ view, the bending angles still satisfy the relationship stated above. This bending angle difference will not depend on the position of the particle where it was created. The reconstruction of the trajectory on the r-ϕ view will not assume a muon coming from the collision point.

Fig. V.9 (left) shows that the relationship between the bending angles differences between station 1 and station 4 vs the p_T is linear. A linear relationship will not require two separated LUT for the p_T assignment unit. Furthermore, the bending angle ϕ_B at station 1 can be as large as the maximum BTI resolution would allow without forcing the use of a low p_T assignment as in the current algorithm.

Fig. V.9 (right) also shows that the proposed algorithm reconstructs the mometum of displaced muon much better than the current algorithm. Compare to Fig. V.7 where the p_T is misassigned.

To demonstrate the working principle we are measuring the bending angle at station MB1 and the bending angle at station MB4. We found that this is the best scenario for reconstructing the p_T of a muon traversing the muon detector. However, a real system will need to use a more elaborate

schema to allow for redundancy in case of a missing detection in MB1 or MB4, and ensure a high signal muon selection efficiency while keeping the background rejection.

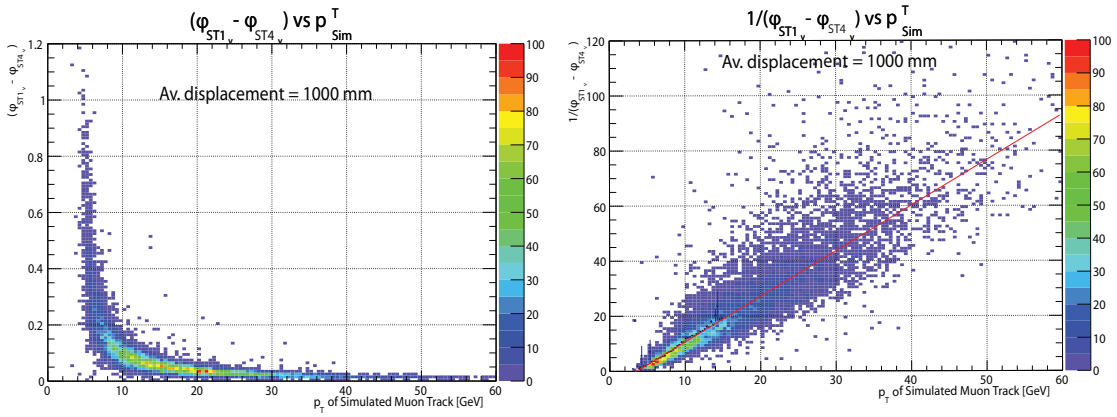

Fig. V.9. $\Delta\phi_{ST1-ST4}$ vs p_T for muons coming from displaced Z_D with cτ up to 1000 mm (left). $1/(\Delta\phi_{ST1-ST4})$ vs p_T shows a linear relationship between the p_T and the inverse difference in bending angle $\Delta\phi_{ST1-ST4}$ (right).

Examples of more bending angle differences between different stations can be found in Fig. V.10. Among the combinations that have a hit in the first station, the difference between station 1 and station 4 produces the best p_T reconstruction. This can be explained by the size of bending in the magnetic field, which accumulates as the muon crosses the return yoke material between the stations. If measurements in either station 1 or 4 are not available, another pairing can be used to estimate p_T: the one with the largest separation in the number of stations is expected to give the best performance.

The implementation of this algorithm in the DTTF will be very similar to the current configuration, except that the Assignment Unit will now require for the difference in the bending angles, $\Delta\phi_B$, instead of the difference in the $\Delta\phi$ coordinates of the hits. It will eliminate most of the problems related to the current algorithm and inherit the strength of a redundant configuration.

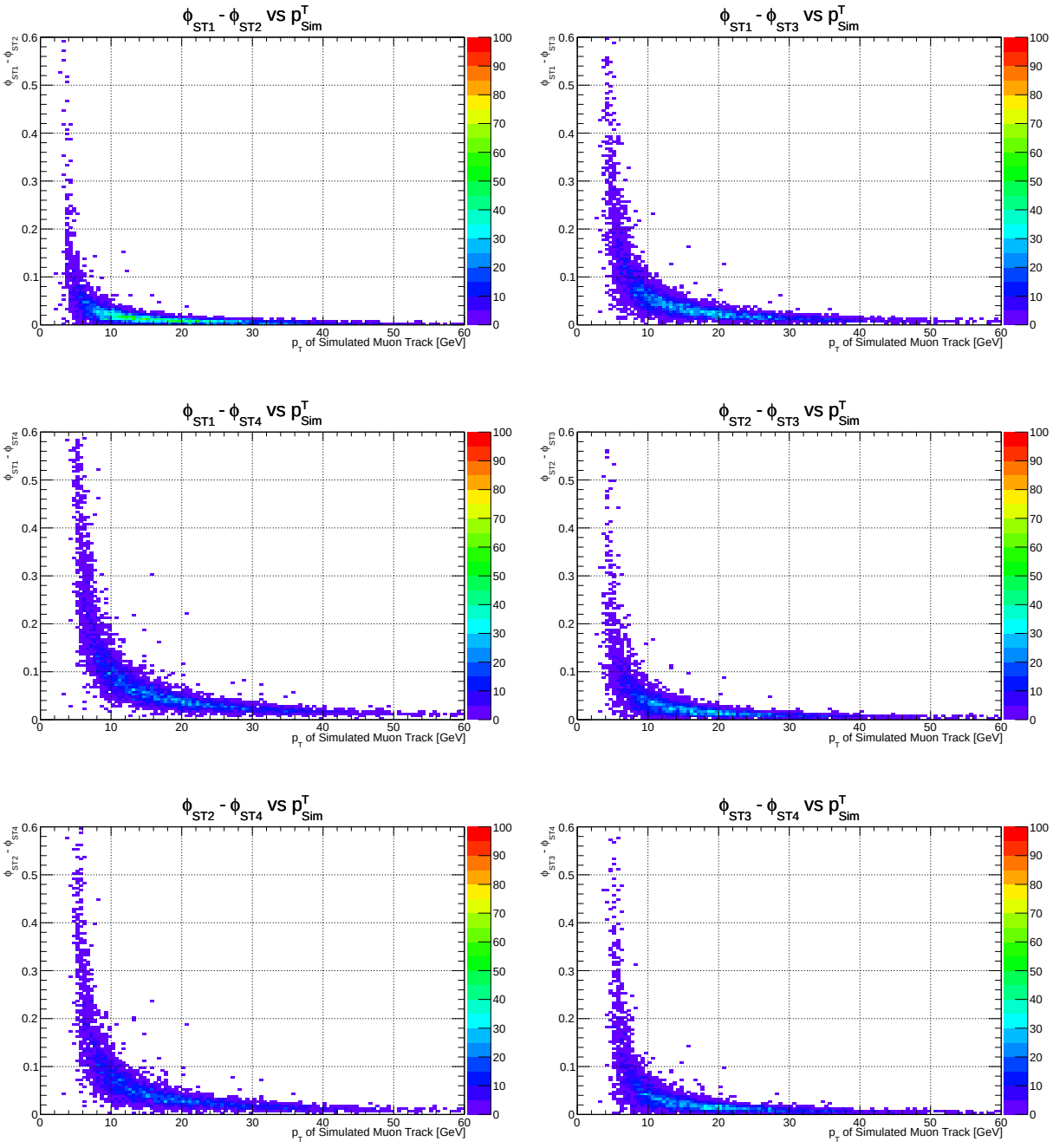

Fig. V.10. $\Delta\phi_B$ measured at different stations vs p_T for muons coming from displaced Z_D with cτ of 1000 mm, showing a clear correlation between the variables. Compare to Fig. IV.4.

V.3 Findings

The proposed algorithm allows a proper p_T reconstruction for muons coming from displaced vertexes without affecting the detection efficiency for muons coming from the interaction point. As opposed to the current configuration, whose efficiency drops as the impact parameter increases, Fig. V.11 shows the p_T efficiency for muons with reconstructed p_T above 20 GeV and different requirements for the impact parameter, $|d_{xy}|$. The efficiency doesn't degrade as the impact parameter increases (compare to Fig. V.5 (right)).

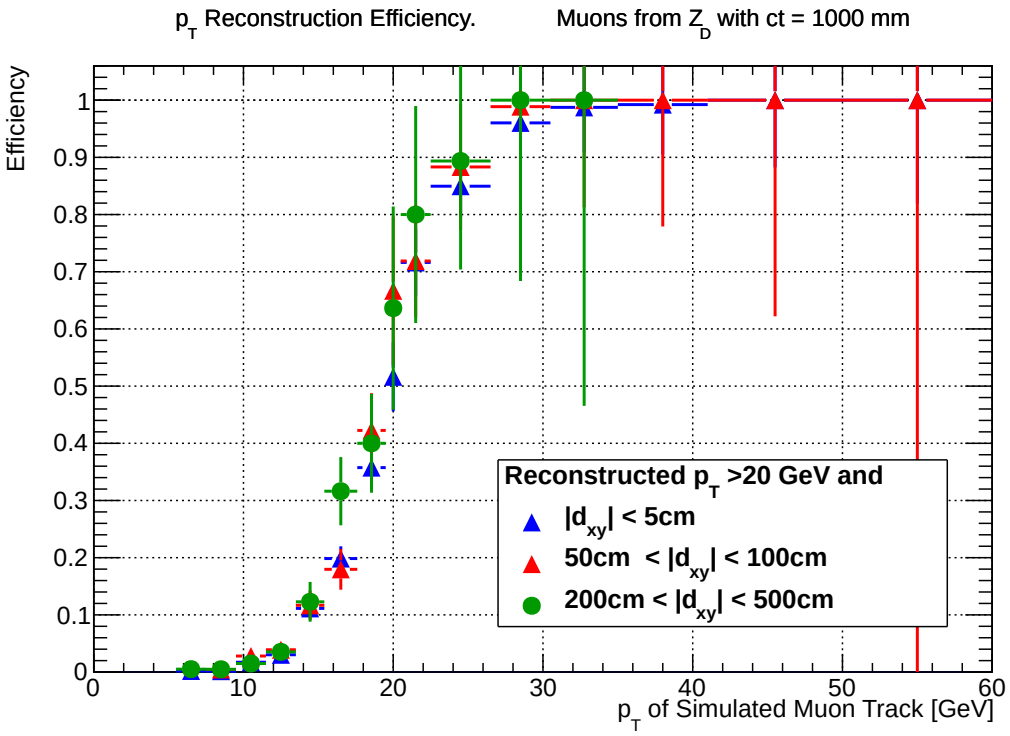

Fig. V.11. Selection efficiency for a trigger configuration requiring reconstructed p_T $\geq$20 GeV of muons.

Fig. V.12 shows the trigger efficiency dependence for several other requirements on reconstructed p_T. A sharp turn on curve is desired to eliminate events below the p_T threshold while effectively detecting all events above that requirement. In the CMS trigger operation the muon momentum

measurement done by the trigger is used to select interesting events. Due to the finite resolution of the measured momentum, the trigger will efficiently select only muons with a true momentum above that measured value. A good trigger has a very high efficiency, close to 100% on the plateau and has a sharp tun on curve. (Compare to Fig. V.5 showing the performance of the current algorithm).

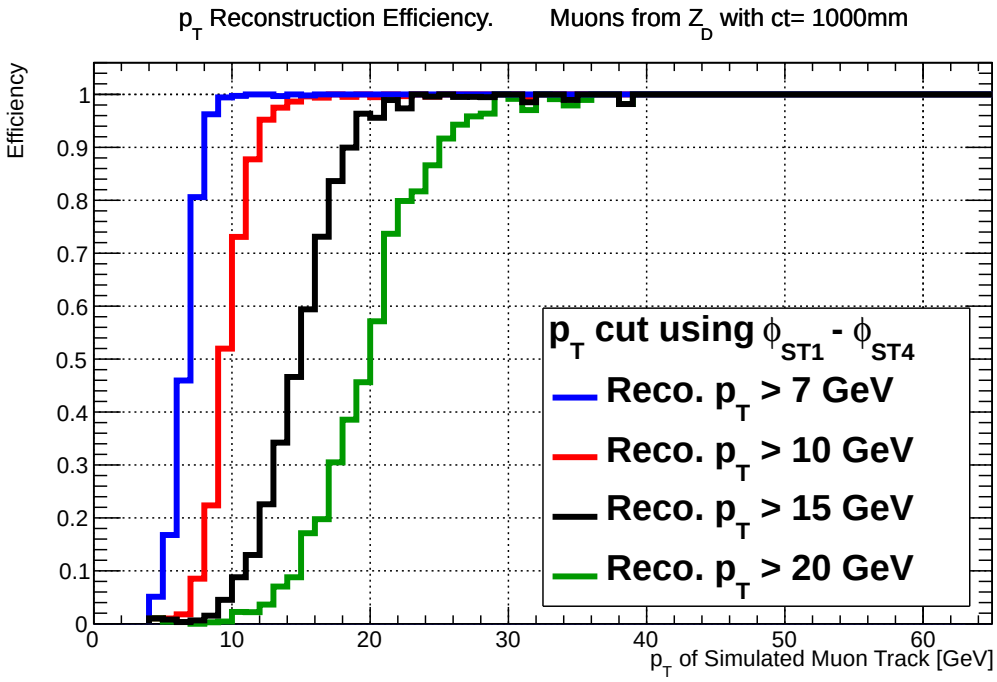

Fig. V.12. Selection efficiency for a trigger configuration requiring different p_T threshold.

Fig. V.13 shows a comparison of expected rates of muon candidates selected by the trigger between the current and proposed algorithm. The rate is estimated for high luminosity LHC operations expected after 2025, shown here for 140 proton-proton interaction per bunch crossing (every 25 ns). Similar performance is expected for the proposed algorithm compared to the current one.

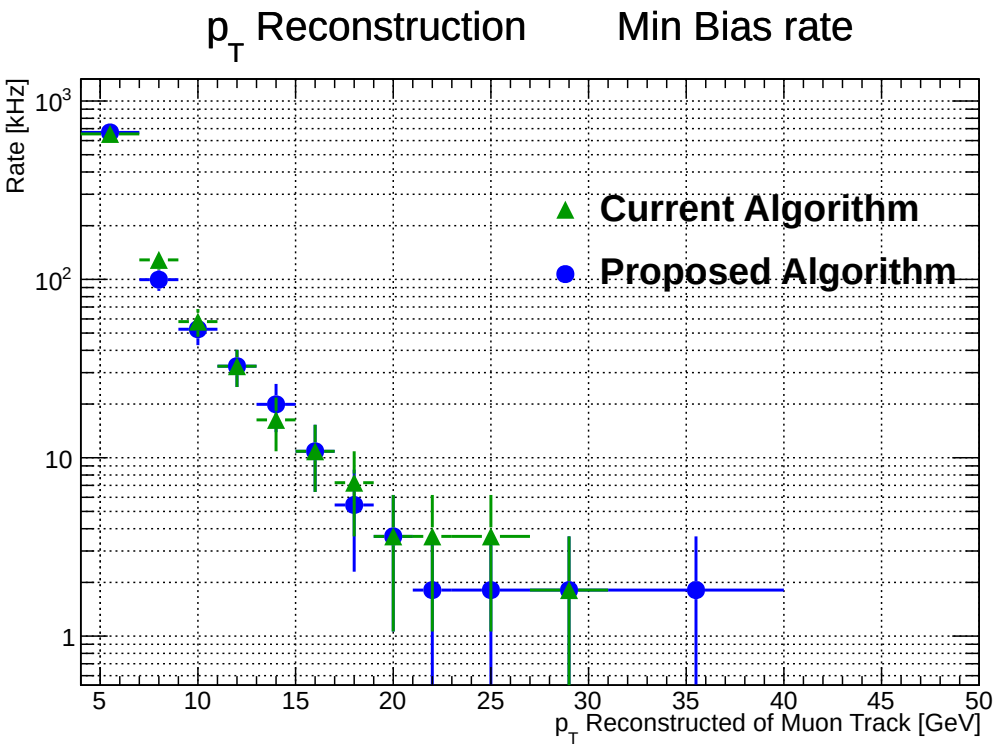

Fig. V.13. Comparison of the trigger rates for the currently used and proposed L1 muon trigger algorithms as a function of the trigger threshold.

CHAPTER VI

CONCLUSIONS

Muons coming from decays of long-lived particles are important signatures in searches for physics beyond the Standard Model. Current selection of displaced muons by the CMS trigger system is identified as a weak point. If nothing is done, CMS can become completely blind to possible signatures of new physics manifesting themselves through production of long lived particles.

We have developed a new algorithm able to reconstruct the transverse momenta of muons regardless of their originating position. The algorithm solves the problem that arises when a neutral particle is formed in the collision and decays into muons after a non vanishind distance without interfering with the reconstruction of muons coming directly from the collision point without displacement.

The new algorithm is shown to deliver at least compatible performance to that of the current algorithm in selection of muons from promp sources. The performance of the proposed algorithm is studied without taking into account inefficiencies in the detector electronics and resolution. Additional tuning of the algorithm will allow further reduction in the triggering rates.

REFERENCES

[1] K.A. Olive et al., Chin. Phys. C, 38, 090001. Particle Data Group. 2014.

[2] Inquiring Minds, *What is the world made of?* 2014: Fermilab. Website

[3] ATLAS Collaboration. *Observation of a new particle in the search for the Standard Model Higgs boson with the ATLAS detector at the LHC*. arXiv:1207.7214

[4] CMS Documentation, *Roadmap for Research and Infrastructures* 2008.

[5] S. Chatrchyan el at, *The CMS experiment at the CERN LHC.* The CMS Collaboration, J. Instrum 3 (2008) S08004

[6] Safonov Alexei et. al. EXO-11-013: *Search for a non-standard-model Higgs boson decaying to a pair of new light bosons in four muon final states* . 2013. arXiv:1210.7619

[7] A. Castaneda et al. *Potential Impact of a New GEM Based Detector on CMS Triggering*. CSC GEM Collaboration, October 2013. arXiv:1310.2074

[8] CMS Software and Physics, Reconstruction and Selection (PRS) Projects, *Physics Technical Document Reading. Volume 1: Detector Performance and Software* 2006: CERN.

[9] Spicas Paris et. al. *The TriDAS Project: The Level-1 Trigger - Technical Design Report* . CMS Collaboration. December, 2000.

[10] Aysen Tatarinov et al. CMS DN-13-022, *Improvements to ME1/1 Trigger Motherboard Algorithm for Operation under High Pile-Up Running Conditions* 2013. CMS Documentation.

[11] The CMS Collaboration. Resonant Muon Jets, *Search for Light Resonances Decaying into Pairs of Muons as a Signal of New Physics*. 2014. arXiv:1106.2375

[12] The CMS Collaboration. *Performance of the CMS Drift Tube Chambers with Cosmic Rays*, 26 Jan 2010. arXiv:0911.4855v2

[13] C. Sergio, R. Attila, S. Paris. *CMS The TriDAS Project : Technical Design Report, Volume 2: Data Acquisition and High-Level Trigger* . CMS Collaboration. Geneva 2002.

[14] E. Mathieson. *Induced Charge Distributions in Proportional Detectors*. Brookhaven National Laboratory, Upton, NY.

[15] S. Agostinelli et a. *GEANT4: A Simulation toolkit*. GEANT4 Collaboration. SLAC-PUB-9350, FERMILAB-PUB-03-339. August 2002.

[16] The CMS Collaboration. *Phase II Upgrade Technical Proposal* . The CMS Collaboration. September 2013.